This is a preprint, the final version is subject to change, of the American Mineralogist (MSA)
Cite as Authors (Year) Title. American Mineralogist, in press.
(DOI will not work until issue is live.) DOI: http://dx.doi.org/10.2138/am-2016-5628

Revision 3

A New EPMA Method for Fast Trace Element Analysis in Simple Matrices

John J. Donovan[1] , Jared W. Singer[2] and John T. Armstrong[3]

[1.] CAMCOR, University of Oregon, Eugene, OR, 97403

[2.] Rensselaer Polytechnic Institute, Troy, New York 12180

[3.] Carnegie Institution for Science, Geophysical Lab, Washington, DC, NW, 20015-1305

Abstract

It is well known that trace element sensitivity in electron probe micro analysis (EPMA) is limited by intrinsic random variation in the x-ray continuum background and weak signals at low concentrations. The continuum portion of the background is produced by deceleration of the electron beam by the Coulombic field of the specimen atoms. In addition to the continuum, the background also includes interferences from secondary emission lines, "holes" in the continuum from secondary Bragg diffraction, non-linear curvature of the wavelength dispersive spectrometer (WDS) continuum and other background artifacts. Typically, the background must be characterized with sufficient precision (along with the peak intensity of the emission line of interest, to obtain the net intensity for subsequent quantification), in order to attain reasonable accuracy for quantification of the elements of interest. Traditionally we characterize these background intensities by measuring on either side of the emission line and interpolate the intensity underneath the peak to obtain the net intensity. Instead, by applying the mean atomic number (MAN) background calibration curve method proposed in this paper for the background intensity correction, such background measurement artifacts are avoided through identification of outliers within a set of standards. We divide the analytical uncertainty of the MAN

This is a preprint, the final version is subject to change, of the American Mineralogist (MSA)
Cite as Authors (Year) Title. American Mineralogist, in press.
(DOI will not work until issue is live.) DOI: http://dx.doi.org/10.2138/am-2016-5628

background calibration between precision errors and accuracy errors. The precision errors of the MAN background calibration are smaller than direct background measurement, if the mean atomic number of the sample matrix is precisely known. For a simple matrix and a suitable blank standard, a high precision blank correction can offset the accuracy component of the MAN uncertainty. Use of the blank-corrected-MAN background calibration can further improve our measurement precision for trace elements compared to traditional off-peak measurements because the background determination is not limited by continuum x-ray counting statistics. For trace element mapping of a simple matrix, the background variance due to major element heterogeneity is exceedingly small and high-precision 2-dimensional background correction is possible.

Introduction

Traditionally electron probe micro analysis (EPMA) has relied upon precise characterization of the continuum intensities adjacent to the emission line of interest for determination of the background under the peak, through interpolation of the off-peak intensities. Recent improvements including new hardware designs with large area Bragg crystals, new software methods implementing exponential and polynomial interpolations to more accurately characterize the curvature of the background, and aggregated spectrometer signals to improve sensitivity, have enabled the EPMA to attain detection limits as low as 2 to 3 PPM in some materials (Donovan et al., 2011).

The traditional off-peak method requires careful selection of background positions to avoid spectral interferences from secondary emission lines near the off-peak intensity positions, and

various continuum artifacts (Kato and Suzuki, 2014). For trace element characterization, the traditional off-peak method generally requires careful study of a wide swath of the emitted continuum spectrum by means of high precision WDS scans, which can be quite time consuming. Such spectrometer scanning techniques are particularly time consuming when WDS scans are performed with a precision similar to subsequent trace quantification measurements, in order to avoid secondary emission lines from other elements when selecting off-peak measurement positions. Unfortunately, even high sensitivity and time consuming wavelength scans may not suffice for some samples where the inhomogeneity of major and/or minor elements may introduce unanticipated off-peak interferences on the pre-specified off-peak positions, which may result in significant inaccuracies in the background determination underneath the peak of interest.

Recent work on a new multi-point background method where multiple high precision off-peak measurements (essentially a sparse high sensitivity wavelength scan combined with a typical quantitative peak intensity measurements), for subsequent "iterative" determination of the optimum background positions based on statistical considerations, has been developed for complex matrices where such off-peak interferences are variable in complex materials such as monazite (Allaz et al., in preparation)

One may also employ time saving techniques such as only measuring the off-peak intensities every N points, sometimes referred to as Nth point backgrounds which is unfortunately inadequate for many trace element applications where the matrix composition (and hence background) varies significantly. But in summary, all these trace element techniques require

careful interpolation from off-peak intensity measurements to obtain the background intensity under the peak. If only we could directly measure the background intensity under the peak and avoid these interpolation, interference and other off-peak measurement artifacts entirely.

In fact, it is possible to measure the background directly beneath the peak without interpolation using the MAN background method. This can also be accomplished either using a blank correction by itself (in the case of simple matrices), or even better, using both a blank correction and the MAN background method described in this paper (in order to deal with differences in composition between the blank standard and the unknown sample). An ideal blank standard has an identical matrix to unknown samples, but is free of trace element contamination. The blank correction is not totally free of spectral artifacts, however the spectral artifacts are similar between unknown and blank.

In this paper we will demonstrate that, at least for materials with a relatively simple matrix such as SiO_2, TiO_2 or $CaMgSi_2O_6$ or $ZrSiO_4$ where one may obtain suitably well characterized standards for use in the so called “blank correction”, we can obtain comparable trace element accuracy to traditional off-peak methods and improved precision in less time than traditional off-peak methods. The MAN background technique was originally intended to apply only to major and minor element characterization (Donovan and Tingle, 1996), but as we will demonstrate, the MAN background method can also be utilized to obtain high precision trace element characterization without off-peak measurements, by simply measuring the on-peak intensities in a number of standard materials that do not contain the element of interest. Influence from standard contaminants and/or spectral artifacts can be observed in the MAN regression curve and

may be subsequently removed as outliers within the set of MAN standards. Trace element accuracy (typically the MAN background method is limited to around 100 to 200 PPM in most silicates and oxides if the blank correction is not utilized), is assured by use of the "blank correction" technique, so that one may obtain similar accuracy with improved precision, and in approximately ½ the acquisition time of off-peak trace element measurements. This MAN background method applies not only to point analyses, but also to quantitative x-ray mapping, where the time savings are particularly significant, and improvements in precision are especially noticeable.

Experimental methods

Data for the $CaMgSi_2O_6$ (diopside) off-peak and MAN comparison were acquired on a Cameca SX51 electron microprobe equipped with 4 tunable wavelength dispersive spectrometers using Probe for EPMA from Probe Software (probesoftware.com). Operating conditions were 40 degrees takeoff angle, beam energy of 20 keV, beam current of 20 nA and the beam diameter was 5 microns. Elements were acquired using analyzing crystals LIF for Fe Kα, Ti Kα, Mn Kα, Ni Kα, K Kα, and TAP for Na Kα and Al Kα. The standards were TiO2 synthetic for Ti Kα, MnO synthetic for Mn Kα, NiO synthetic for Ni Kα, Labradorite (Lake Co.) for Na Kα, Orthoclase MAD-10 for K Kα, Al Kα, and Magnetite U.C. #3380 for Fe Kα. The on-peak counting time was 20 seconds and the off peak counting time was also 20 seconds (in total) for all elements. The off peak correction method was linear interpolation for all elements and the MAN background intensity data was calibrated and continuum absorption corrected for K Kα, Fe Kα, Ti Kα, Na Kα, Al Kα, Mn Kα, Ni Kα and all intensities were corrected for dead time.

Standard intensities were corrected for standard drift over time and interference corrections were applied to Fe for interference by Mn (Donovan et al., 1993) and a $CaMgSi_2O_6$ matrix was specified by difference. The matrix correction method was $\phi(\rho z)$ and the mass absorption coefficients dataset was Henke (LBL, 1985). The $\phi(\rho z)$ method algorithm utilized was Armstrong/Love Scott.

Data for the SiO_2 point analyses and quantitative x-ray maps were acquired on a Cameca SX100 electron microprobe equipped with 5 tunable wavelength dispersive spectrometers using Probe for EPMA, Probe Image for x-ray map acquisitions and re-processed using CalcImage software also from Probe Software. Operating conditions were 40 degrees takeoff angle, beam energy of 15 keV, beam current was 100 nA, and the beam diameter was 10 microns for the point analysis and 1 um for the x-ray maps. Elements were acquired using analyzing crystals LLIF for Fe Kα, LPET for Ti Kα, PET for K Kα, and TAP for Al Kα, Na Kα. The standards were TiO2 synthetic for Ti Kα, Nepheline for Na Kα, and Orthoclase MAD-10 for K Kα, Al Kα, and Magnetite U.C. #3380 for Fe Kα. The off- peak correction method was linear interpolation for Fe Kα, K Kα, Na Kα, average for Al Kα, and exponential for Ti Kα (generally one should use a polynomial or exponential interpolation for Al Kα in SiO_2 because the Al Kα peak is on the tail of the Si Kα line, but the blank correction deals with this issue effectively, so the fit method is a moot point in this case). Unknown and standard intensities were corrected for dead time. Oxygen was calculated by cation stoichiometry and included in the matrix correction. Si was calculated by difference from 100%. The matrix correction method was $\phi(\rho z)$ by Armstrong/Love Scott. The SiO_2 blank by laser ablation ICP-MS gave 1.4 PPM Ti and AA gave 15 PPM Al and 6 PPM Fe.

Data for the $ZrSiO_4$ point analyses were obtained using a synthetic zircon from John Hanchar (Memorial University), and quantitative x-ray maps using SIMS Oxygen standard AS3, all acquired on a Cameca SX100 electron microprobe equipped with 5 tunable wavelength dispersive spectrometers using Probe for EPMA for the standard intensities, Probe Image for x-ray map acquisition and re-processed using CalcImage software also from Probe Software. Operating conditions were 40 degrees takeoff angle, beam energy of 20 keV, beam current was 100 nA, and the beam diameter was 5 microns for the point analyses and 1 micron for the x-ray map acquisitions. Elements were acquired using analyzing crystals PET for Th Mα, Y Lα, LPET for U Mα, P Kα, PET for Th Mα, Y Lα, and TAP for Hf Mα. The standards were UO_2 for U Mα, $ThSiO_4$ (Thorite) for Th Mα, $HfSiO_4$ (Hafnon) for Hf Mα, and YPO_4 (USNM 168499) for P Kα and Y Lα. The on-peak and off-peak counting time for point analyses was 640 seconds for all elements. The off-peak correction method was linear for Th Mα, U Mα, Y Lα, and exponential for P Kα and Hf Mα. Unknown and standard intensities were corrected for dead time. Standard intensities were corrected for standard drift over time. Point analysis results are the average of 5 points. Si, Zr and O were specified for the matrix correction. The quantitative blank correction was utilized based on a synthetic zircon from Lynn Boatner (Oak Ridge National Laboratory) which was characterized by laser ablation ICP-MS measurements by Alan Koenig (USGS Denver) and yielded 15 PPM Hf, 25 PPM Y and below detection limit (<1ppm) for U and Th. Phosphorus was not characterized due to difficulties with the LA-ICP-MS method for this element. The matrix correction method was the $\phi(\rho z)$ algorithm by Armstrong/Love Scott.

Revision 3

MAN Background Corrections

An alternative background correction method known as the mean atomic number (MAN) background correction, based on Kramer's Law (Kramers, 1923),

$$\mathrm{N(E)} = \mathrm{iZ}[(E_O - E)/E]dE$$

has been in use for over 20 years now. Although originally designed for EPMA monochromators that cannot be "detuned" off-peak, the method has been extended and improved for all types of Bragg spectrometers by the use of multiple standards and linear or polynomial regression of the measured on-peak intensities in standards that do not contain the element of interest. Further improvement has been accomplished by correction for continuum absorption (Armstrong, 1988), based on a modified form of the relationship between Z-bar and intensity by Ware and Reed which includes a correction for continuum absorption by the specimen (Ware and Reed, 1973) where I(E) is the background intensity as a function of i, Z, E_O, E, and *f(x)*, where i is the beam current, Z is the average atomic number, E_O is the beam energy, E is the energy of the emission and *f(x)* is the matrix correction all integrated over the energy range:

$$\mathrm{I(E)} = \mathrm{iZ}\left\{\left[\frac{(E_O - E)}{E}\right] f(x)\right\} dE$$

The continuum absorption correction improves accuracy and regression precision, since each standard material utilized in the MAN regression curve will have different absorption effects on the particular (on-peak) photon energy of interest.

MAN Background Method Iteration

It should be noted that because the MAN background intensities are recalculated during each iteration of the matrix correction, we require two iteration loops in our quantification method.

One loop for the normal matrix correction (whatever physics algorithm that might be), and a second outer iteration loop for all the compositionally dependent corrections such as: MAN backgrounds, quantitative spectral interferences, and compound area-peak factors for chemical shifts and peak shape changes.

This double iteration loop allows the program to "refine" the calculated MAN background as the composition of the unknown converges (MAN background correction of standard intensities is trivial since their compositions are already known and hence their average Z is fixed). For unknowns the process is performed in several steps. First the on-peak intensities for a number of standards not containing the element of interest and covering a range of atomic number for the standards and anticipated unknown compositions are acquired by the analyst (or reloaded from a previous MAN calibration). Second the on-peak intensities on the standards used for the MAN calibration are corrected for continuum absorption by the simple relation:

$$I_{COR} = I_{RAW} * ZAF^{S}$$

Where I_{COR} is the absorption corrected intensity for the MAN standard, and ZAF^{S} is the absorption correction for the standard composition (note that the ZAF^{S} term here is the inverse of the *f(x)* term in Ware and Reed's expression). This "virtual" intensity MAN calibration curve which has been corrected for continuum absorption, is then stored for subsequent use for MAN background correction of unknown compositions. During the iterated matrix correction of the unknown intensities, we initially assume an arbitrary Z-bar for the unknown, and then calculate the background intensity from our previously acquired and stored "virtual" MAN intensity regression. This calculated average Z is then improved as the composition converges during the

matrix iteration. Finally we de-correct the calculated background intensity for the continuum absorption associated with the actual unknown composition as seen here:

$$I_{RAW} = {I_{COR}}/{ZAF^{U}}$$

where ZAF^{U} is the absorption term for the unknown composition undergoing iteration. The I_{RAW} background intensity is then simply subtracted from the measured unknown on-peak intensity to obtain the background corrected intensity for the unknown composition. This calculation proceeds until the composition (and hence average Z) converges, and a proper background correction has been applied.

The measured standard intensities should be corrected for continuum absorption to improve regression accuracy and precision, especially at sub 100 to 200 PPM levels. As mentioned above, a continuum absorption "de-correction" must also be applied to the regressed MAN background intensity due to the fact that the unknown specimen intensity will generally have a different specimen matrix than the standards utilized for the MAN calibration curve. The effect of the continuum absorption is most significant for low energy emission lines from elements such as sodium, magnesium, etc. as seen in figures 1 and 2. For higher energy emission lines from such elements as potassium and iron, the continuum absorption correction effect is decreased, but still significant for best accuracy as seen in figures 3 and 4. Note that because the differences in continuum absorption primarily contributes towards a larger variance as opposed to an absolute change in the intensity regression fit, the absence of a continuum absorption correction is a minor effect except in cases of low energy emission lines such as Na Kα, Mg Kα, etc.

Revision 3

Precision of MAN Background Method

The MAN background method is capable of higher precision than traditional off-peak background determinations particularly when the measured matrix Z-bar variance from the major elements is small. That is, the MAN Z-bar variance for trace element analysis is typically small because it is based on either measurements of high intensity x-rays from the major elements or matrix specification by difference or fixed concentration elements. Also the MAN background method can achieve a low correlation variance if suitably known and pure reference materials are used and the above continuum absorption correction is appropriately applied. In contrast, off-peak background intensities are relatively weak signals with associated poor counting statistics, therefore interpolation from off peak intensity measurements imbues an intrinsically larger variance.

To highlight the improved precision of the MAN background method, we compare the propagated net intensity variance for off-peak and for MAN background correction methods derived from the generalized variance equation for function *f* of *i* principal variables: The total variance of a function or an operation (*f*) is the square root of the summation of all partial differential equations multiplied by each constituent variance, for *i* principal variables as seen here:

$$\sigma_f(i) = \sqrt{\sum_i \left(\frac{\partial f}{\partial i}\sigma_i\right)^2}$$

For any method of background correction (off peak, MAN, or Nth point), the background intensity (B) is subtracted from the peak intensity (P) for the net intensity (I_{net}):

$$I_{net}(P, B) = P - B$$

248 The partial derivatives in the case of subtraction are negligible, and the variance equation
249 becomes,

$$\sigma_{net} = \sqrt{(1 * \sigma_P)^2 + (-1 * \sigma_B)^2}$$

250 and we simplify to the familiar expression for net intensity variance:

$$\sigma_{net} = \sqrt{\sigma_P^2 + \sigma_B^2}$$

251 Traditionally the peak and background variance is determined directly from counting statistics,
252 and for a single measurement this error estimate does not include other sources of variance such
253 as standard homogeneity, spectrometer movement, beam current measurement, environmental
254 stability, and so on. For linear off peak background interpolation (B_{OFF}), the interpolation in
255 slope-intercept form is,

$$B_{OFF}(x, m, b) = m * x + b$$

256 There are three principal variables, namely *x* spectrometer coordinate, *m* background slope, and *b*
257 the interpolation intercept. The propagated off-peak background variance ($\sigma_{B,\,OFF}$) is,

$$\sigma_{B_{OFF}} = \sqrt{\left(\frac{\partial B_{OFF}}{\partial x}\sigma_x\right)^2 + \left(\frac{\partial B_{OFF}}{\partial m}\sigma_m\right)^2 + \left(\frac{\partial B_{OFF}}{\partial b}\sigma_b\right)^2}$$

258 The partial derivatives of B_{OFF} are,

$$\frac{\partial B_{OFF}}{\partial x} = m \quad \frac{\partial B_{OFF}}{\partial m} = x \quad \frac{\partial B_{OFF}}{\partial b} = 1$$

259 The off-peak background variance (σ_B) simplifies to the following,

$$\sigma_{B_{OFF}} = \sqrt{(m * \sigma_x)^2 + (x * \sigma_m)^2 + (1 * \sigma_b)^2}$$

260 The propagated off-peak background variance is commonly ignored, because two-point
261 interpolation allows no estimates of slope and intercept variance (σ_m and σ_b). However in the
262 case of replicate measurements using off-peak background corrections, each of the above terms

arise naturally from the measurement process. The first term (m* σ_x) indicates that spectrometer reproducibility (σ_x) is exacerbated when the background is increasingly sloped. The correlation variance, terms $(x^* \sigma_m)^2$ and $(\sigma_b)^2$, aggregate many sources of variance that would affect the quality of the linear regression including systematic error when the true background is not linear. When the propagated off-peak background variance is neglected (along with factors affecting the on peak variance), the error estimates for a single analysis will be arbitrarily small compared to the real fluctuations of replicate measurements. If off peak correlation variance were possible to estimate (such as for multi-point, off peak), the weak background intensities may lead to large correlation variance without significant time investment in background characterization.

The propagated MAN background variance ($\sigma_{B,\,MAN}$) is derived from a background intensity correlation function (B_{MAN}), which may be specified according to the operator of best fit, including linear or 2nd order polynomial. For Kramer's Law the expected dependence of background intensity on Z-bar is linear, however curvature well-fit by a 2nd order polynomial is often observed. For the linear case, the MAN background intensity is correlated with Z-bar (the average atomic number) in the form of a line with slope (m) and intercept (b):

$$B_{MAN}(\overline{Z}, m, b) = m * \overline{Z} + b$$

Thus the MAN background variance is,

$$\sigma_{B_{MAN}} = \sqrt{\left(\frac{\partial f}{\partial \bar{Z}}\sigma_{\bar{Z}}\right)^2 + \left(\frac{\partial f}{\partial m}\sigma_m\right)^2 + \left(\frac{\partial f}{\partial b}\sigma_b\right)^2}$$

For the linear case the partial derivatives are

$$\frac{\partial B_{MAN}}{\partial \bar{Z}} = m \quad \frac{\partial B_{MAN}}{\partial m} = \bar{Z} \quad \frac{\partial B_{MAN}}{\partial b} = 1$$

Combining these terms we arrive at an intermediate result,

Revision 3

$$\sigma_{B_{MAN}} = \sqrt{(m * \sigma_{\bar{Z}})^2 + (\bar{Z} * \sigma_m)^2 + (1 * \sigma_b)^2}$$

which emphasizes the basic dependencies of the MAN background variance on Z-bar and correlation variance. For example, as Z-bar becomes large, the MAN background variance depends more strongly on the slope variance (σ_m); likewise as the slope becomes large, the MAN background variance depends strongly on Z-bar variance ($\sigma_{Z\text{-}bar}$). The slope and intercept variances are calculated from the residuals of the best-fit (not derived here) and practically the MAN correlation variances depend on factors including the purity of the standards used to generate the MAN background correlation, on the absence of on-peak interferences, and on application of the absorption correction (discussed in the previous section). As for off-peak methods, the propagated correlation variance may aggregate numerous sources of error (both random and systematic).

The Z-bar value is obtained from concentration weighted averaging, since we are estimating the average strength of the Coulombic field of the atoms composing the specimen matrix (Donovan and Pingitore, 2002), which is in turn of course determined by the number of electrons in the specimen matrix atoms. And since A/Z is approximately a constant over the periodic table it provides a reasonable weighting for average atomic number in compounds. Hence the mean atomic number (Z-bar) is calculated from the summation of the atomic numbers multiplied by the weighted fractions (c_i) for all elements *i* in the total composition:

$$\bar{Z} = \sum_i c_i * Z_i$$

The sum of the concentration weighted fractions must sum close to one to ensure the completeness of the matrix Z-bar calculation. The partial derivatives of the Z-bar operator are,

Revision 3

$$\frac{\partial \bar{Z}}{\partial c_i} = Z_i \quad \frac{\partial \bar{Z}}{\partial Z_i} = c_i$$

It follows that the Z-bar variance is a series for i=1 to i=n elements in the total composition:

$$\sigma_{\bar{Z}} = \sqrt{\left(\frac{\partial \bar{Z}}{\partial c_1}\sigma_{C_1}\right)^2 + \left(\frac{\partial \bar{Z}}{\partial Z_1}\sigma_{Z_1}\right)^2 + \cdots \left(\frac{\partial \bar{Z}}{\partial c_n}\sigma_{C_n}\right)^2 + \left(\frac{\partial \bar{Z}}{\partial Z_n}\sigma_{Z_n}\right)^2}$$

Substituting the simplified partial derivatives we obtain,

$$\sigma_{\bar{Z}} = \sqrt{\left(Z_1 * \sigma_{C_1}\right)^2 + \left(c_1 * \sigma_{Z_1}\right)^2 + \cdots \left(Z_n * \sigma_{C_n}\right)^2 + \left(c_n * \sigma_{Z_n}\right)^2}$$

An individual atomic number Z_i is a physical constant (therefore, $\sigma_{Zi} = 0$), and ($c_i * \sigma_{Zi}$) terms drop out:

$$\sigma_{\bar{Z}} = \sqrt{\left(Z_1 * \sigma_{C_1}\right)^2 + \cdots \left(Z_n * \sigma_{C_n}\right)^2}$$

$$\sigma_{\bar{Z}} = \sqrt{\left(\sum_i Z_i * \sigma_{C_i}\right)}$$

The above equation shows that elements having large atomic numbers have a disproportionate effect on the Z-bar variance. However, it is important to note that regardless of Z_i's absolute value, major elements will contribute the largest portion of the concentration-weighted variance. Individual concentration weighted variances (σ_{ci}) for elements *i* to *n* are obtained by direct analysis or in the case of a simple sample matrix, the major element concentration (c_{major}) and major element variances may be inferred by difference from *i* trace element concentrations:

$$c_{major} = 1 - \sum_i c_i$$

The average Z variance of measured matrix elements (those elements not by fixed concentration or specified by difference) is the following expression:

Revision 3

$$\sigma_{C_{major}} = \sqrt{\left(\sum_i \sigma_{C_i}^2\right)}$$

Bringing the various statements together, the propagated MAN background variance in the case of linear correlation is,

$$\sigma_{B\ \ MAN} = \sqrt{\left(m * \sqrt{\sum_i \left(Z_i \sigma_{C_i}\right)^2}\right)^2 + (\bar{Z} * \sigma_m)^2 + (1 * \sigma_b)^2}$$

This full propagated error expression with the MAN correlation variance terms will be referred to as "Model A" in the discussion. Now if the MAN correlation variance is considered an accuracy issue (see discussion in the Accuracy Versus Precision in the MAN Background Method section for further explanation), the variance on the MAN background intensity simplifies to this expression which only includes the variance in the specimen matrix average Z and the slope of the MAN regression:

$$\sigma_{B\ MAN} = m * \sqrt{\sum_i \left(Z_i \sigma_{c_i}\right)^2}$$

Note that the above expression, without the MAN regression precision terms, is referred to as "Model B" in subsequent discussion.

Before we proceed it may be instructive to consider the time savings and precision increase in the case of so called Nth point off-peak backgrounds where the analyst measures the off-peak background only every N acquisitions where N is greater than 1. The idea being that subsequent acquisitions only measure the on-peak intensities and simply re-utilize the initial off-peak measurement. In this case, the background intensity is treated as a constant (for those replicate measurements) and hence the background intensity variance on these subsequent measurements

is zero. The tradeoff is that the background intensity accuracy of these subsequent analyses is unknown since the background is no longer being measured directly. Thus, the Nth point background correction is only suitable for highly homogeneous materials. The time savings (approaching ½) may be achieved if the background is measured only once by the Nth point background correction for a set of on peak analyses. Increase in precision can be rationalized practically, because spectrometer movement can be minimized and time-dependent sources of variance may also be mitigated through time savings. Mathematically, we are subtracting a constant background value for replicate peak measurements; therefore when using an Nth point background method, the observed replicate net intensity variance includes only the on-peak variance.

In a similar manner the MAN method does not directly measure the background intensity for every measurement, but instead calculates the background for the unknown in question based on the measured composition (average atomic number) of the unknown data point (unlike the Nth point background method, the MAN background method automatically handles changes in matrix composition), and the previously acquired MAN calibration curve, which is based on on-peak intensity measurements on standards that do not contain the element(s) of interest. In other words, a single MAN calibration curve is utilized for many replicate measurements, and since for a given average Z, the same background intensity will be obtained, the variance of replicate calculations is not precisely zero, but instead very close to zero. In general we can improve our sensitivity by approximately $\sqrt{2}$ when P ≈ B because the MAN background variance term approaches zero in the case of a fixed matrix and is only slightly larger in the case of a measured matrix, because the MAN background determination is dominated by the major element

intensities. At the same time reduce our total x-ray integration time by some 50% because we are only measuring the on-peak intensities for our trace elements.

Use Of The Blank Correction To Improve Accuracy For Trace MAN Analyses

Although we are able to improve precision and reduce acquisition time by means of the MAN background correction, we must still deal with the issue of accuracy at the trace level since there will always be systematic artifacts at some trace level in the x-ray continuum spectrum. To improve accuracy of our MAN background modeling, due to the possible imperfect nature of the reference materials and the continuum modeling used in the MAN regression, the "blank" correction can be applied for further improvement in trace element accuracy in specimens (SiO_2, TiO_2, $ZrSiO_4$, etc.) when a blank [or non-zero concentration] secondary standard with a matching matrix is available. A true blank (zero; below detection limit) is more preferred than low-level reference materials; if a non-zero concentration reference material is used, then the overall accuracy of EPMA is predicated on the systematic errors of another technique. Fortunately for specimens with simple matrices such as SiO_2, TiO_2, $CaMgSi_2O_6$, $ZrSiO_4$, etc., we can easily improve MAN background accuracy by use of the "blank" correction method previously described. Although originally intended for off-peak measurements, where secondary Bragg reflection and sample absorption edges can produce artifacts as large as 50 PPM, the blank correction allows the MAN background correction to achieve accuracy similar to the precision with which the blank standard was measured.

As discussed, the MAN method is based on measuring the on-peak intensities for several standards which do not contain an element of interest, but also cover the range of average atomic number (Z-bar) for the unknowns and standards being utilized. The typical Z-bar range for oxides and silicates is generally from 10 to 20 and therefore simple oxides such as MgO, Al_2O_3, SiO_2, TiO_2 and MnO or NiO are usually ideal for such purposes. Therefore these MAN calibration standards can be any material with appropriate Z-bars which do not contain the element of interest (on-peak interferences can be avoided with a simple review of the regression fit since, interferences or unsuspected contamination for that matter, will always show as outliers above the general curve of the regression).

The accuracy of the MAN background correction can be ascertained by acquiring the complete on and off peak intensities and calculating the background correction using both off-peak and MAN methods on the same dataset, since the MAN background correction simply ignores the off-peak data, if it was acquired. A comparison between off-peak and MAN methods performed on a $CaMgSi_2O_6$ (diopside) standard candidate is shown in Table 1, where it can be seen that the concentration differences between the off-peak and MAN methods are less than the reported variance of the measurements. For example off-peak measurements of Na yields 160 PPM Na and -10 PPM K, but using the MAN background corrections on the same intensity data, we obtain essentially the same concentration results (170 PPM Na and 10 PPM K), that is within the precision of the measurements.

A further comparison of synthetic SiO_2 is seen in Table 2a and 2b where again the off-peak and MAN background corrections produce results that are within 100 PPM of each other. Table 2c

shows the results for the MAN analyses where the blank correction has been applied from our SiO_2 standard, and it can be seen that the accuracy is now equal to or better than the measured variance when compared to ICP-MS analyses.

For a further test, we acquired both traditional off-peak and the MAN background corrected point intensities for Ti and Al in a natural quartz (Audetat) in separate acquisitions. Results acquired using both off-peak background and MAN background methods are shown for Ti in Figure 5 and for Al in Figure 6. Note that these point analyses were acquired separately as both off-peak and MAN acquisitions, separated in time (proxy to line numbers). Of course this accuracy improvement generally only pertains to specimen matrices with relatively simple compositions for which a suitable "blank" standard containing a zero (or known non-zero) concentration is available. But this may include pure metals, pure oxides, simple silicates and sulfides, etc., so a large number of materials can benefit from this trace element method.

X-ray Mapping and MAN Background Corrections

Although the use of the MAN background correction method combined with the blank correction for trace element point analyses results in acquisition times that are approximately ½ that of normal off-peak measurements (while improving precision and maintaining accuracy similar to the precision of the on-peak intensity), similar time savings results from the use of the MAN background correction for x-ray mapping. This is because one need only acquire the on-peak

intensity map, since the background is calculated based on the MAN fit to point acquisitions of standards not containing the element of interest as described above.

Mapping results (based three x-ray map acquisitions for each sample: the on-peak intensity pixel map, the high side pixel intensity map and the low side pixel intensity map- note that MAN results utilize only the on-peak intensity map), are shown for pure synthetic SiO_2, first with off-peak map pixel intensities interpolated and subtracted from the on-peak pixel intensities in figure 7a, using the same raw intensity acquisition dataset on the SiO_2 sample for both background correction methods (with the on-peak pixel intensities corrected using the MAN calibration curve from standards applied in figure 7b). Note the significant improvement of the MAN background intensity precision. In fact the variance of the MAN background intensities is due only to the variance of the trace elements effect on the average Z calculation. Again, if we consider Nth point statistics, the background variance for Nth point intensities is zero because the background intensity is constant, but accuracy suffers since the Nth point background method does not account for changes in composition as the MAN method does automatically.

It should be noted that typical x-ray mapping integration times per pixel a few seconds or less are generally of insufficient sensitivity to warrant the use of the blank correction in silicates and oxides, although it can be applied if a suitable blank standard can be obtained for the material in question if necessary. In other words, only when the per pixel x-ray mapping sensitivity begins to approach typical MAN accuracy of around 100 to 200 PPM (in silicates and oxides), is the blank correction step actually necessary for x-ray mapping.

444 In the case of the SiO_2 background intensity maps shown in fig. 7b, one can see that the MAN
445 background intensity variances are several orders of magnitude smaller than a direct
446 measurement of the backgrounds using the off-peak method in fig. 7a. In fact the measured
447 concentrations shown in figs. 8a and 8b, are well below the detection limit of approximately 100
448 PPM as shown in the detection limit maps for the same SiO_2 specimen for all elements measured
449 in figures 9a and 9b. It is evident that the calculated pixel detection limits for off-peak
450 measurements shown in figure 9a has a greater variation compared to the pixel detection limits
451 for MAN measurements due to the variance as seen in the interpolated off-peak intensity maps
452 (fig. 7a). On the other hand, the MAN detection limit maps show more constant detection limits
453 which is as expected due to the MAN background being essentially a constant for the given
454 average atomic number (composition of SiO_2 gives ~10.4 Z-bar).
455
456
457 **Application to Amethyst and Zircon**
458 Figures 9c and 9d compare traditional off-peak x-ray maps for synthetic SiO_2 with the same
459 measured intensity data processed using MAN background and utilizing only the on-peak
460 intensities. This results in improved precision in approximately ½ the acquisition time (assuming
461 trace acquisitions where the on and off peak pixel integration times are roughly equal).
462 The improvement in trace sensitivity shown above for SiO_2 and amethyst are significant, but
463 with an average Z of roughly 10, the continuum intensities are relatively low and the peak to
464 background ratios quite good.
465

466 However, for the case of zircon ($ZrSiO_4$), with an average atomic number of approximately 24,
467 we can expect a larger correction for background intensity. Again we acquired point analyses
468 and x-ray maps on two synthetic zircons and a natural zircon (SIMS oxygen isotope standard
469 AS3) for U, Th, Y, P and Hf. Figures 10 and 11 shows results for blank corrected point analyses
470 of two synthetic zircons, the first grown by John Hanchar at Memorial University and the
471 second, grown by Lynn Boatner at Oak Ridge National Laboratory for U, P, Hf and Th. The only
472 observable statistically result, was P at approximately 80 PPM higher in the Hanchar material,
473 than the Oak Ridge Laboratory material.
474
475 Figure 12a and 12b compares the calculated background intensities for x-ray maps (based three
476 x-ray map acquisitions for each sample: the on-peak intensity pixel map, the high side pixel
477 intensity map and the low side pixel intensity map- note that MAN results utilize only the on-
478 peak intensity map), calculated for 4 of these elements after applying both the off-peak and
479 MAN background correction methods using the same raw intensity acquisition dataset on the
480 zircon sample for both background correction methods for the quantitative results in 12c and
481 12d. Again we can see that the variance of the off-peak measured and interpolated background
482 intensities are significantly larger than the same data calculated using the MAN method (using
483 only the measured on-peak intensities and the MAN calibration curve standards of synthetic
484 $MgSiO_4$, $FeSiO_4$, $MnSiO_4$, $CoSiO_4$, $NiSiO_4$, $PbSiO_4$ and $ThSiO_4$). Finally, figures 13a and 13b
485 compare detection sensitivity for both background correction methods.
486
487 Background intensity and elemental concentration maps are shown in fig. 14 for the natural
488 zircon SIMS oxygen standard where some trace heterogeneity can be seen in the Hf map. The

489 improvement in precision for the MAN method (and the maintaining of accuracy) is easily seen
490 in the last figure (fig. 15), where the U concentration profile across the concentration maps in
491 figures 14c and 14d are shown for both the off-peak and MAN methods calculated from the same
492 acquisition dataset.
493
494
495 **Accuracy Versus Precision in the MAN Background Method**
496 When we consider traditional off-peak measurements we obtain a variance from the on-peak
497 measurement and a variance from the off-peak measurement. When these measured on-peak and
498 high and low off-peak intensities are subtracted from each other, the errors add in quadrature as
499 described above. In the case of Nth point off-peak measurements the variances are solely due to
500 the on-peak variances and the off-peak intensity is a constant. As is the case with traditional and
501 Nth point off-peak methods, the MAN background method variance is also dominated by the on-
502 peak statistics, but with a minor contribution from the major element statistics and the slope of
503 the MAN regression, rather than the Gaussian statistics of the continuum. In the case where these
504 major elements are measured, the MAN variance depends on the major element counting
505 statistics and in the case where these major elements are simply specified as fixed concentrations
506 or by difference, only the trace element variances contribute towards the determination of
507 average atomic number variance.
508
509 Some analysts have pointed out that there must be a precision or error associated with the MAN
510 regression as derived for Model A, yet we do not observe this correlation variance in replicate
511 measurements. We can see this by comparing actual measured background intensity variances

512 from off-peak measurements with a fixed matrix, MAN measurements with a fixed matrix and
513 MAN measurements with measured matrix elements) with the calculated sensitivities for the off-
514 peak and MAN methods respectively from our MAN variance model as seen in table 3. In table
515 3a we compare the average and standard deviation for the calculated off-peak background
516 intensities from off-peak (analogous to fig. 12a), that is, measured and interpolated under the
517 peak, with the calculated background variance by assuming Gaussian statistics on the peak and
518 background and adding them in quadrature as discussed previously. As one can see, the
519 calculated and modeled off-peak intensity variances are quite similar.
520
521 For comparison with MAN background intensity statistics, we can examine table 3b which
522 shows the average and standard deviation of the measured and regressed MAN background
523 intensities obtained by calculation of the average Z and MAN regression curve, when the matrix
524 major elements are fixed (analogous to fig. 12b), with the modeled MAN sensitivities from our
525 MAN sensitivity/variance expressions, for both model A (using the full MAN variance
526 expression including the terms for the MAN regression precision), and model B (using the
527 modified MAN variance expression without the MAN regression precision terms). As can be
528 seen, by including the MAN regression precision terms in the MAN variance model (model A),
529 we obtain variances which are approximately 100 times greater than the variances of the
530 calculated MAN background intensities from our quantification procedures. On the other hand,
531 using model B, we obtain predicted MAN background variances that agree quite well with MAN
532 background measurements. The reason the MAN variances are so small in table 3b compared to
533 the off-peak background variances in table 3a, is that the matrix elements (Zr, Si and O) were
534 specified as a fixed concentration (statistically similar to the Nth point constant background

This is a preprint, the final version is subject to change, of the American Mineralogist (MSA)
Cite as Authors (Year) Title. American Mineralogist, in press.
(DOI will not work until issue is live.) DOI: http://dx.doi.org/10.2138/am-2016-5628

535 method). This can easily be seen in the elemental concentration data for U in fig. 15 where the
536 off-peak and MAN calculated concentrations are compared. In this case of fixed matrix
537 elements, the only contribution to the average Z variance is from the measured trace elements.
538 As expected, specifying the matrix as $ZrSiO_4$ by difference from 100 percent (not shown), yields
539 almost exactly the same measured MAN intensities and variances as using a fixed compositional
540 matrix.
541
542 In table 3c we again compare the measured and calculated variances, but this time with Zr and Si
543 measured analytically and oxygen calculated by stoichiometry. In this case where the major
544 elements are measured, the actual MAN background variance is slightly larger than with the
545 fixed or by difference compositional matrix as seen in 3b. But again, model A produces
546 predicted MAN background variances that are approximately 10 greater than we observe in the
547 calculated MAN background intensities, while using model B the measured and calculated MAN
548 background intensity variances are again very similar, thus demonstrating the validity of our
549 MAN sensitivity model without including the MAN regression precision terms, as unintuitive as
550 this may seem.
551
552
553 Another way to consider the issue of accuracy and precision in the MAN method is to realize
554 that if one re-measures intensities utilized for the MAN regression curve, the fit coefficients will
555 be slightly different, giving a slightly different background intensity for the same average Z,
556 when compared to the previous MAN calibration. However, this intensity difference between
557 subsequent MAN regressions merely represents a systematic accuracy error, since each single

new MAN regression fit will repeatedly produce the same high precision intensity for a given composition (and hence average Z) for every new unknown measurement, resulting in improved precision when it is subtracted from the on-peak measurement. Indeed, if we did re-measure the MAN calibration curve intensities for every point analysis and every x-ray map pixel, then we would need to include the MAN regression precision in our sensitivity calculations. But in fact, we do not re-measure the MAN intensities for every unknown measurement and instead correct for MAN accuracy using the blank correction.

A principal challenge for users of the MAN background method is limiting the unknown Z-bar variance through high precision analysis of major elements or by restriction to simple matrices (with fixed concentration or by difference major elements). Maximizing the accuracy of the MAN regression depends on primary standards that are pure, homogeneous and do not contain the element of interest and proper correction of continuum absorption. In practice, a few simple metals or oxides such as MgO, Al_2O_3, SiO_2, TiO_2, MnO and NiO will suffice for calibrating the continuum for a variety of emission lines in most silicates and oxides. If such standards are used, then the correlation variances will be inherently minimized and accuracy improved by avoiding MAN standards that interfere with the on-peak measurement positions.

Calculation of Detection Limits With The MAN Background Method

Because the MAN background intensity variation does not follow Gaussian statistics, we cannot base our sensitivity concentration of detection limit (CDL) calculations on traditional expressions which only utilize the background variance. Instead, we must add our calculated

MAN background variance to our on-peak variance as previously described to obtain a net concentration variance. There are several methods traditionally utilized to calculate the minimum detection limit (CDL) for off-peak intensity measurements. One method is to assume that three times the variance of the raw photon intensity, expressed as a concentration and corrected for matrix effects yields a 99% confidence estimate of detection limits (Scott et al., 1995) as seen here:

$$C_{CDL} = \frac{3\sqrt{I_B}}{I_S}$$

However, because the variances of the calculated MAN background intensities do not follow Gaussian statistics, we cannot simply assume this for the MAN detection limit. In the limit as the background variance approaches zero, this definition of the CDL approaches zero (infinitely low). Instead we will need to utilize the net intensity variance for the MAN sensitivity calculation. Based on the off-peak net intensity variance expression we will propose that the MAN net intensity variance is similarly expressed as:

$$\sigma_{MAN_{net}} = \sqrt{\sigma_P^2 + \sigma_B^2}$$

Where in this case, σ_P is the calculated MAN intensity under the peak, and σ_B is the calculated MAN background variance from the model B MAN variance expression. In the case of a fixed composition matrix, e.g., $ZrSiO_4$ by difference (see table 3b), the value of σ_B approaches zero, so we can compare the situation where we have an normal peak variance and a zero background variance (as we would in the case of Nth point off-peaks), and find that as σ_B approaches zero our net intensity statistics are improved by a factor of $\sqrt{2}$ or roughly 1/3 as the MAN background variance approaches zero. Therefore, at least in the case of our fixed composition matrix, we

should expect to obtain MAN detection limits that are roughly 1/3 better than traditional off-peak measurements.

Comparing off-peak detection limits calculated by assuming 3 times the background variance, we find that using 2 net intensity variances we obtain an MAN CDL that is approximately 1/3 better which is not surprising since the MAN background variance term is close to zero. Figures 9a and 9b for SiO_2 and figures 13a and 13b for $ZrSiO_4$ demonstrate this.

Finally see table 4 for a comparison of blank and non-blank corrected measurement results for the Oak Ridge synthetic zircon for off-peak, Nth Point and MAN background methods where it can be seen that the application of the blank correction results in an insignificant increase in the absolute standard deviation, which is due to the fact that the blank correction itself is small compared to the total background, and the blank standard calibration (as is the case with the MAN standard intensities), is measured only once, but then applied repeatedly to subsequent replicate datasets to improve accuracy. Again, if we did re-measure the blank correction for every point acquisition or x-ray map pixel, we would indeed need to include the blank correction variance in the trace element sensitivity for all background methods. But since we do not generally re-measure the blank standard for every point or pixel acquisition, we are merely limiting our blank accuracy to the precision of the blank standard measurement.

This is a preprint, the final version is subject to change, of the American Mineralogist (MSA)
Cite as Authors (Year) Title. American Mineralogist, in press.
(DOI will not work until issue is live.) DOI: http://dx.doi.org/10.2138/am-2016-5628

Conclusions

For simple matrices where an appropriate blank specimen is available (that is, a material with a similar matrix to the unknown, which contains a known zero or non-zero level of the element of interest), the use of MAN background calibration curve modeling for high accuracy trace element analysis is easy, automatic and can reduce acquisition times by as much as 50%.

This situation is more common than one might think as it can be applied to the analysis of trace elements in pure metals, pure oxides, pure carbides, etc., and even simple compounds such as relatively pure silicates, sulfides and carbonates, where a suitable matrix matched "blank" standard can often be obtained to ensure accuracy at trace levels.

At the same time, the MAN background intensity is essentially a constant (related only to the variance and slope of the average atomic number determination), if the matrix is specified by fixed concentration or by difference, or has a very small variance when the major elements are measured. This means that because the variance of the background measurement can be close to zero in such simple matrices, the analytical precision is further improved by approximately 30% or more depending on the physics details, again in approximately ½ the acquisition time.

This is a preprint, the final version is subject to change, of the American Mineralogist (MSA)
Cite as Authors (Year) Title. American Mineralogist, in press.
(DOI will not work until issue is live.) DOI: http://dx.doi.org/10.2138/am-2016-5628

640 **Acknowledgments**

641 We would like to thank our informal reviewers Paul Carpenter at Washington University and
642 Michel Jercinovic at the University of Massachusetts at Amherst for valuable suggestions and
643 critical comments and feedback. We also acknowledge funding from NSF EAR-0345908 and the
644 Murdoch Foundation for purchase of the Cameca SX100 EPMA instrument. We additionally
645 acknowledge the gracious donation of synthetic zircons from Lynn Boatner at Oak Ridge
646 National Laboratory and John Hanchar at Memorial University. The synthetic quartz and zircon
647 were characterized for trace elements by Allan Koenig at the USGS in Denver, Colorado. The
648 natural zircon SIMS standard was provided by Dylan Colon and Ilya Bindeman at the University
649 of Oregon. The authors would also like to thank two anonymous reviewers for their helpful
650 suggestions and comments.

651

652

References

Allaz, J., Williams, M.L., Jercinovic, M.J., and Donovan, J.J. (in preparation) Multipoint Background Method: Gaining precision and accuracy in electron microprobe trace element analysis. To be submitted to Chemical Geology

Armstrong, J.T. (1988) Quantitative Analysis of Silicate and Oxide Materials: Comparison of Monte Carlo, ZAF, and Procedures, Microbeam Analysis, 239-246

Donovan, J.J., Snyder, D.A., and Rivers, M.L. (1993) An Improved Interference Correction for Trace Element Analysis, Microbeam Analysis, 2, 23-28

Donovan, J.J., and Tingle, T. (1996) An Improved Mean Atomic Number Background Correction for Quantitative Microanalysis, Journal of Microscopy and Microanalysis, 2, 1-7 http://www.probesoftware.com

Donovan, J.J., and Pingitore, N. (2002) Compositional Averaging of Continuum Intensities in Multi-Element Compounds. Microbeam Analysis

Donovan, J.J., Lowers, H.A., and Rusk, B.G. (2011) Improved Electron Probe Microanalysis of Trace Elements in Quartz, American Mineralogist, 96, 274-282

Kato, T., and Suzuki, K. (2014) “Background holes” in X-ray spectrometry using pentaerythritol (PET) analyzing crystal, Journal of Mineralogical and Petrological Sciences, 109, 151-155

Kramers, H. (1923) On the theory of X-ray absorption and the continuous X-ray spectrum, Philosophical Magazine, 46, 836

Scott, V.D., Love, G., and Reed, S.J.B. (1995) Quantitative Electron-Probe Microanalysis, 2nd. Ed., In Ellis Horwood Series Physics and its Applications, 105

Ware, N.G., and Reed, S.J.B. (1973) Background corrections for quantitative electron microprobe analysis using a lithium drifted silicon X-ray detector. Journal of Physics E: Scientific Instruments, 6, 286-288

This is a preprint, the final version is subject to change, of the American Mineralogist (MSA)
Cite as Authors (Year) Title. American Mineralogist, in press.
(DOI will not work until issue is live.) DOI: http://dx.doi.org/10.2138/am-2016-5628

687 **Tables**

Element	X-ray	Crystal	Off-Peak Wt.%	Std. Dev.	MAN Wt.%
K	Kα	PET	-0.001	0.004	0.001
Fe	Kα	LIF	0.05	0.015	0.051
Ti	Kα	LIF	-0.001	0.008	0.003
Na	Kα	TAP	0.016	0.009	0.017
Al	Kα	TAP	0.026	0.006	0.014
Mn	Kα	LIF	0.007	0.008	-0.005
Ni	Kα	LIF	0.002	0.009	-0.003

688

689 Table 1. $CaMgSi_2O_6$ (diopside) standard analyzed for traces as an "unknown" using traditional
690 off-peak intensity background corrections, compared to MAN background corrections (20 keV,
691 20 nA, 5 um beam, 20 second on-peak integration time, 20 seconds off-peak integration time,
692 average of 10 points). Note that the differences in the concentrations between off-peak and MAN
693 are within the measured variances.

694

695

This is a preprint, the final version is subject to change, of the American Mineralogist (MSA)
Cite as Authors (Year) Title. American Mineralogist, in press.
(DOI will not work until issue is live.) DOI: http://dx.doi.org/10.2138/am-2016-5628

	Ti	Fe	Al	K	Na	Si	O	Total
Average:	**-.00095**	**.00154**	**.00294**	**.00018**	**.00021**	**46.740**	**53.256**	**100.000**
Std Dev:	**.00105**	**.00139**	**.00097**	**.00092**	**.00108**	**.001**	**.00060**	**.000**
%Rel SD:	-116.10	89.75	32.95	523.27	525.57	-	-	-

Table 2a **Off-peak analysis** of synthetic SiO_2, 15 keV, 100 nA, 10 um beam, 180 seconds on-peak and 180 seconds off-peak, average of 5 points. **Without the blank correction applied.**

	Ti	Fe	Al	K	Na	Si	O	Total
Average:	**-.00300**	**-.00487**	**.00438**	**-.00128**	**-.00402**	**46.748**	**53.261**	**100.000**
Std Dev:	**.00034**	**.00146**	**.00053**	**.00042**	**.00062**	**.001**	**.00046**	**.000**
%Rel SD:	-11.43	-29.99	12.09	-32.99	-15.52	-	-	-

Table 2b **MAN analysis** of standard SiO_2, 15 keV, 100 nA, 10 um beam, 180 seconds on-peak average of 5 points. **Without the blank correction applied**. Note the significantly improved standard deviations in the results for the MAN background correction compared to the traditional off-peak method seen in table 2a.

	Ti	Fe	Al	K	Na	Si	O	Total
Average:	**.00013**	**.00059**	**.00150**	**-.00001**	**.00052**	**46.741**	**53.2564**	**100.000**
Std Dev:	**.00034**	**.00146**	**.00053**	**.00042**	**.00063**	**.001**	**.00046**	**.000**

Table 2c **MAN analysis** of standard SiO_2, 15 keV, 100 nA, 10 um beam, 180 seconds on-peak, average of 5 points. **With the blank correction applied** from the SiO_2 bulk standard to itself, the accuracy now is similar to the precision of the measurements. ICP-MS: Ti 1.42 PPM. AA: Fe 6 +/- 3 PPM, Al 15 +/- 5 PPM, Na 5 +/- 3 PPM.

This is a preprint, the final version is subject to change, of the American Mineralogist (MSA)
Cite as Authors (Year) Title. American Mineralogist, in press.
(DOI will not work until issue is live.) DOI: http://dx.doi.org/10.2138/am-2016-5628

709 Table 3a

	Th	Hf	U	P	Y
Average	**.226061**	**2.02225**	**.611455**	**.320043**	**.113804**
Std Deviation	**.028376**	**.142604**	**.128880**	**.037488**	**.021821**

710

Off-peak Model	**.027325**	**.081837**	**.044766**	**.032520**	**.019335**

711

712 Comparison of off-peak background measurement and interpolation for all background intensity
713 map pixels (analogous to Fig. 17) with calculated off-peak variance (average of all pixels)
714 assuming Gaussian statistics (square root of raw photon intensity). Note that the variation from
715 the measured off-peak intensities and the calculated variance model is excellent except for Hf
716 and U where the measured variation is somewhat larger. This larger variation for Hf and U could
717 be due to trace concentration variation in the standard material.
718
719
720 Table 3b

	Th	Hf	U	P	Y
Average	**.254557**	**2.04241**	**.630875**	**.280978**	**.113875**
Std Deviation	**.000348**	**.001509**	**.002499**	**.000904**	**.000156**

721

MAN Model (A)	**.025887**	**.076575**	**.026831**	**.017200**	**.006861**
MAN Model (B)	**.000328**	**.001510**	**.000612**	**.000265**	**.000095**

722

723 Comparison of MAN background calculations for all background intensity map pixels with fixed
724 matrix (analogous to Fig. 18) (Zr 49.764, Si 15.322, O 34.914 wt.%) with the calculated MAN
725 background variance (average of all pixels) from our model. Model A is using the full MAN
726 variance expression with the terms for the MAN regression precision and model B is the
727 modified MAN variance expression without the MAN regression precision terms. Note that since
728 the $ZrSiO_4$ matrix is specified and therefore constant, the average atomic number variance is
729 minimal for the MAN regression curve. However, model A which includes the MAN regression
730 precision terms of the MAN variance expression, results in predicted background intensity
731 variances that are approximately 100 times larger than observed in the actual data, while model
732 B, without the MAN regression precision terms, produces predicted variances which are in
733 excellent agreement with the actual MAN background intensity variances.
734
735
736 Table 3c

	Th	Hf	U	P	Y
Average	**.254586**	**2.04253**	**.630940**	**.281020**	**.113894**
Std Deviation	**.000812**	**.002682**	**.002897**	**.001754**	**.000683**

737

MAN Model (A)	**.027446**	**.083754**	**.029741**	**.018462**	**.007315**
MAN Model (B)	**.001886**	**.008685**	**.003521**	**.001526**	**.000549**

738

739 Comparison of MAN background calculations for all background intensity map pixels with a
740 measured $ZrSiO_4$ matrix. Again model A is using the full MAN variance expression with the
741 terms for the MAN regression precision and model B is the modified MAN variance expression
742 without the MAN regression precision terms. Since the major elements are actually measured

here (relative to a $ZrSiO_4$ standard), the average atomic number variance is dominated by the major element concentration variation. Therefore the measured and predicted (modeled) variances are somewhat larger than the fixed matrix variances seen in table 3b as expected. However, model A which includes the MAN regression precision terms of the MAN variance expression, results in predicted background intensity variances that are approximately 10 times larger than observed in the actual data, while model B, without the MAN regression precision terms, produces predicted variances which are in excellent agreement with the actual MAN background intensity variances.

Revision 3

Off-peak, No blank		Th WT%	Hf WT%	U WT%	P WT%	Y WT%
	Average	0.002138	0.01171	0.013602	-0.00505	-0.00947
	Std Dev	0.006832	0.005244	0.005994	0.000706	0.005989

		Th WT%	Hf WT%	U WT%	P WT%	Y WT%
Off-peak, Blank	Average	0	0.001499	0.000001	0.000001	0.002501
	Std Dev	0.006832	0.005243	0.005994	0.000706	0.005989

		Th WT%	Hf WT%	U WT%	P WT%	Y WT%
Nth Point, No Blank	Average	0.001715	0.007501	0.018374	-0.00611	-0.00796
	Std Dev	0.004528	0.003775	0.001211	0.000376	0.002593

		Th WT%	Hf WT%	U WT%	P WT%	Y WT%
Nth Point, Blank	Average	0	0.001499	0.000002	0.000001	0.002501
	Std Dev	0.004529	0.003775	0.001211	0.000376	0.002593

MAN, No blank		Th WT%	Hf WT%	U WT%	P WT%	Y WT%
	Average	-0.05026	0.014599	-0.04495	0.028541	0.025386
	Std Dev	0.00447	0.00417	0.001219	0.000387	0.002595

MAN, Blank		Th WT%	Hf WT%	U WT%	P WT%	Y WT%
	Average	-0.00092	0.001398	-0.00071	-0.00005	0.00222
	Std Dev	0.004469	0.004169	0.001219	0.000387	0.002595

Table 4

Comparison of measured variances in replicate measurements of Oak Ridge zircon at 20 keV, 100 nA, average of 5 points for off-peak and MAN measurements, with and without the blank correction. As expected the measured variances (Std Dev) are almost identical between the blank and non-blank measurements. Note also that the Nth Point and MAN background methods give similar standard deviation results in about the same acquisition time, the difference being that the Nth Point background method cannot handle compositional heterogeneity, while the MAN background method can.

This is a preprint, the final version is subject to change, of the American Mineralogist (MSA)
Cite as Authors (Year) Title. American Mineralogist, in press.
(DOI will not work until issue is live.) DOI: http://dx.doi.org/10.2138/am-2016-5628

Revision 3

762 **Figures**

763

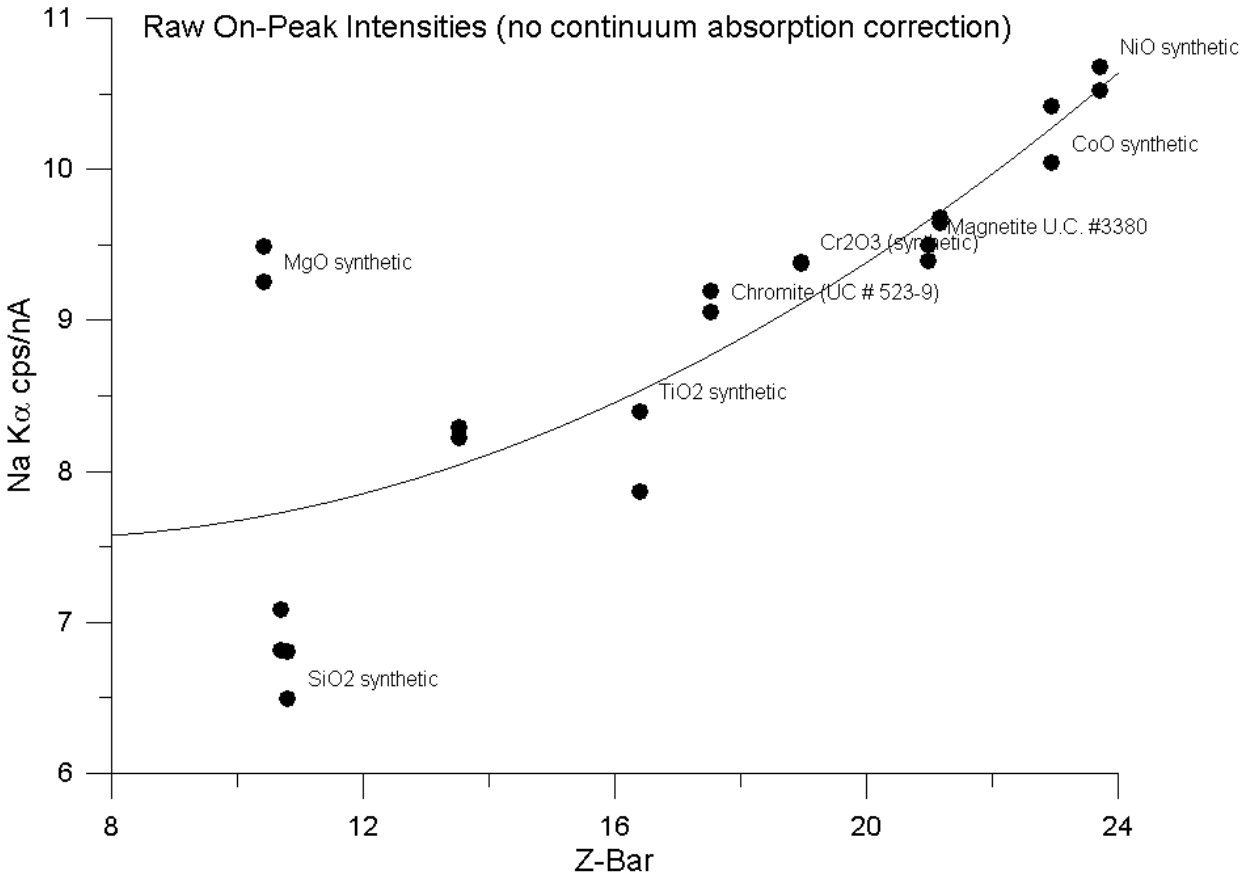

764

765

766 Fig 1. MAN (on-peak) background calibration curve for Na Kα, (20 keV, 20 nA, 5 um, 20

767 seconds integration time using TAP crystal) uncorrected for continuum absorption. 2nd order

768 polynomial fit yields an average relative deviation of approximately 8.5%.

769

770

771

772

This is a preprint, the final version is subject to change, of the American Mineralogist (MSA)
Cite as Authors (Year) Title. American Mineralogist, in press.
(DOI will not work until issue is live.) DOI: http://dx.doi.org/10.2138/am-2016-5628

Revision 3

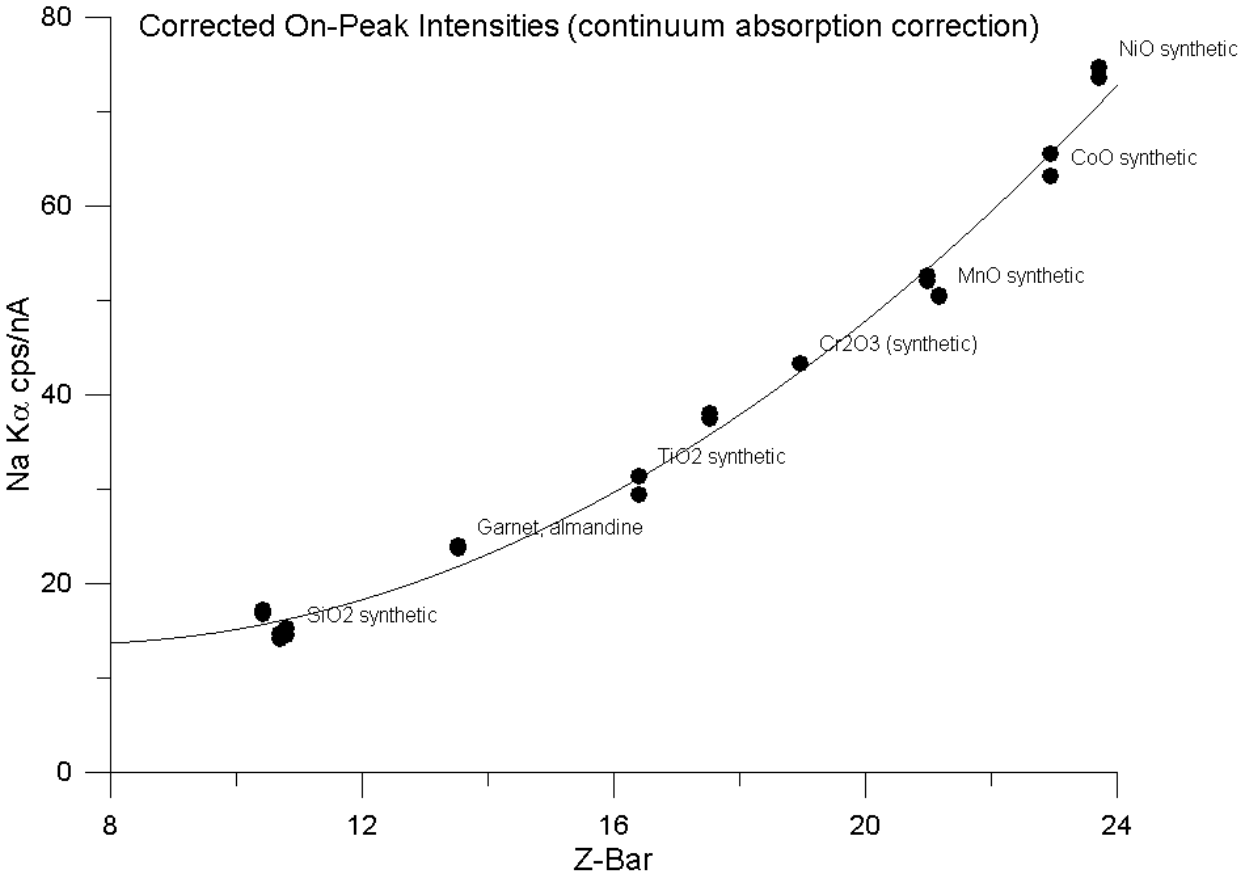

773

774 Fig 2. MAN (on-peak) background calibration curve for Na Kα, (20 keV, 20 nA, 5 um, 20
775 seconds integration time using TAP crystal) corrected for continuum absorption. 2nd order
776 polynomial fit yields an average relative deviation of approximately 5.5%.

777

This is a preprint, the final version is subject to change, of the American Mineralogist (MSA)
Cite as Authors (Year) Title. American Mineralogist, in press.
(DOI will not work until issue is live.) DOI: http://dx.doi.org/10.2138/am-2016-5628

Revision 3

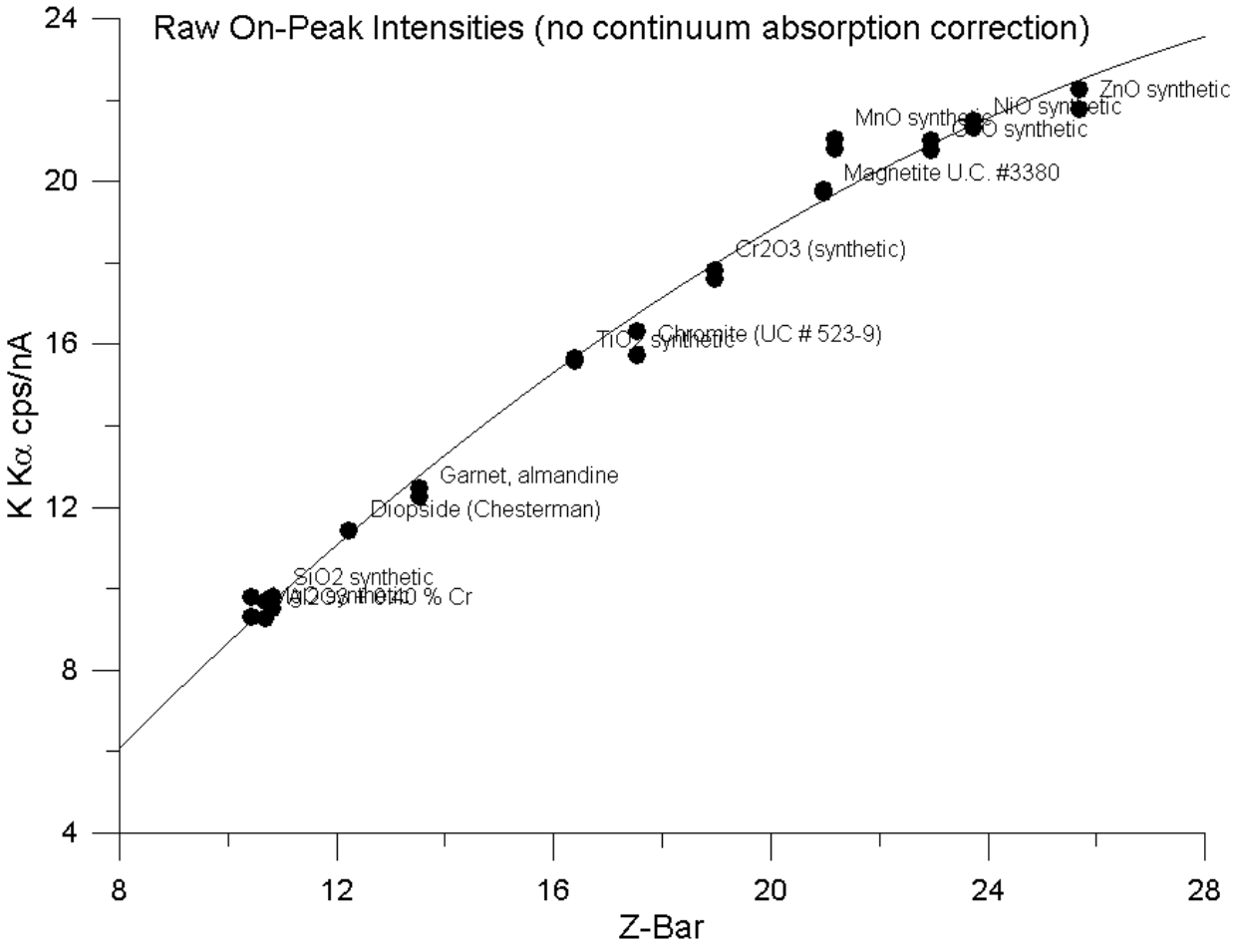

Fig 3. MAN (on-peak) background calibration curve for K Kα, (20 keV, 20 nA, 5 um, 20 seconds integration time using PET crystal) uncorrected for continuum absorption. 2nd order polynomial fit yields an average relative deviation of approximately 2.6%.

Revision 3

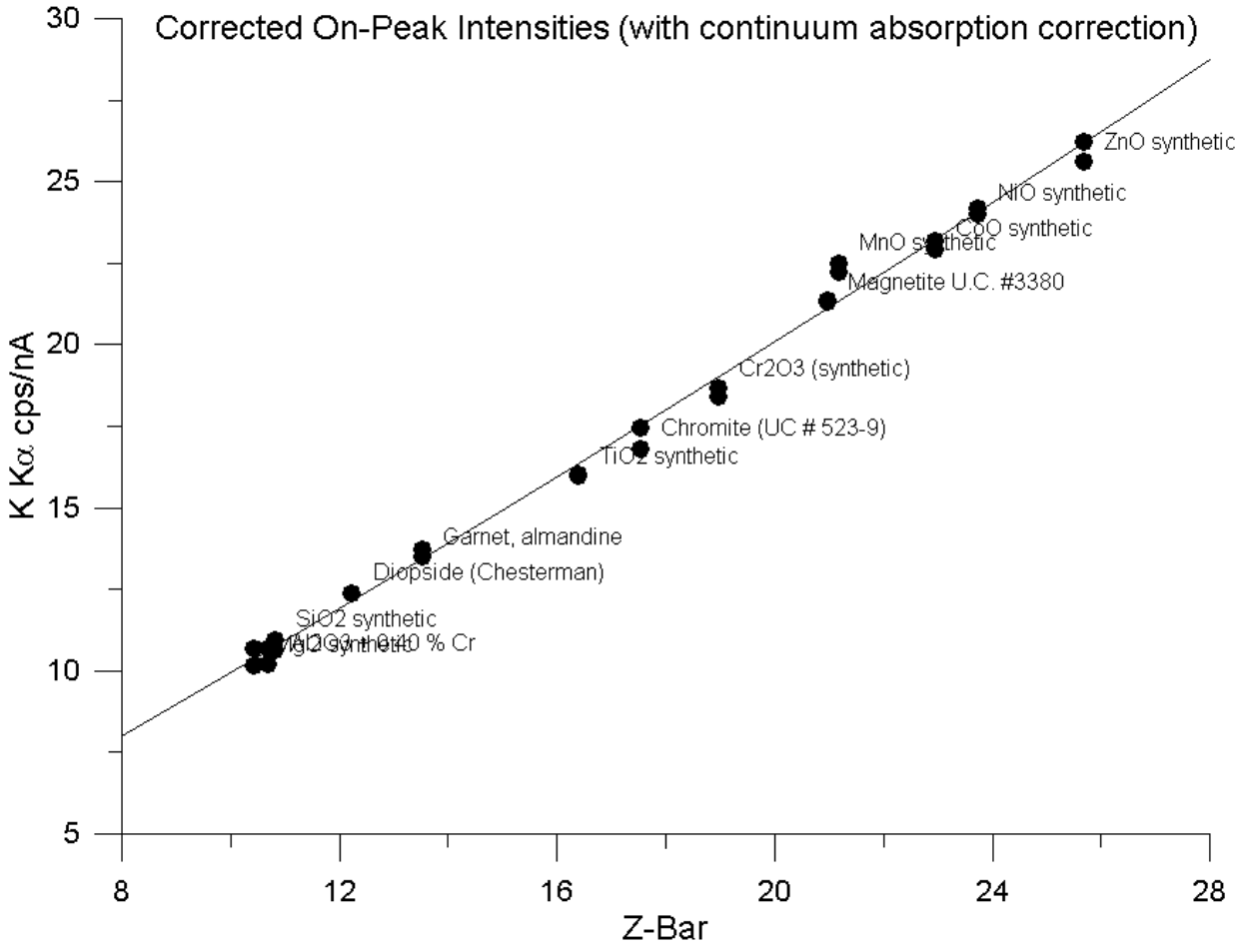

783

784 Fig 4. MAN (on-peak) background calibration curve for K Kα, (20 keV, 20 nA, 5 um, 20
785 seconds integration time using PET crystal) corrected for continuum absorption. 2nd order
786 polynomial fit yields an average relative deviation of approximately 2.1%.

This is a preprint, the final version is subject to change, of the American Mineralogist (MSA)
Cite as Authors (Year) Title. American Mineralogist, in press.
(DOI will not work until issue is live.) DOI: http://dx.doi.org/10.2138/am-2016-5628

Revision 3

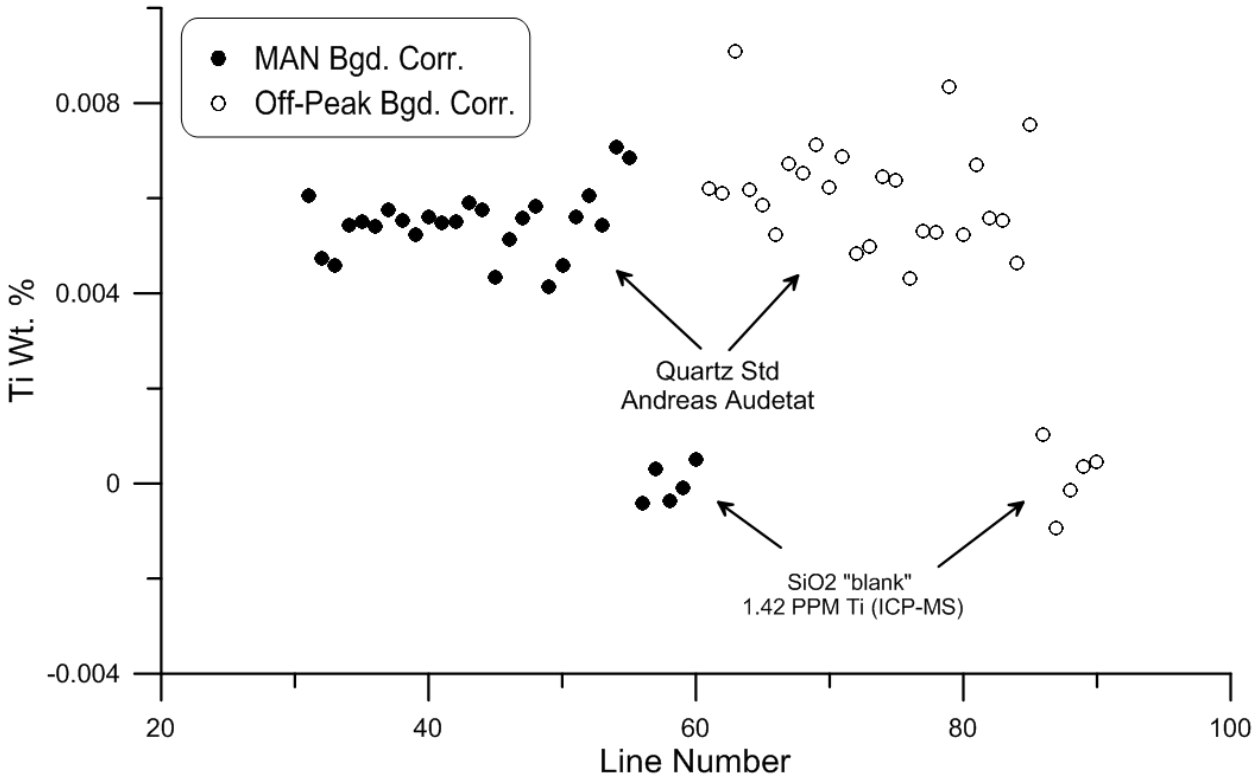

Fig 5. Ti wt.% in Audetat natural quartz standard. MAN vs. Off-Peak, Ti Kα (LIF/LLIF), 20 keV, 100 nA, 10 um, 200 secs on-peak, (200 secs off-peak), Both datasets are aggregates from 2 spectrometers and blank corrected. “Line number” refers to the acquisition order.

This is a preprint, the final version is subject to change, of the American Mineralogist (MSA)
Cite as Authors (Year) Title. American Mineralogist, in press.
(DOI will not work until issue is live.) DOI: http://dx.doi.org/10.2138/am-2016-5628

Revision 3

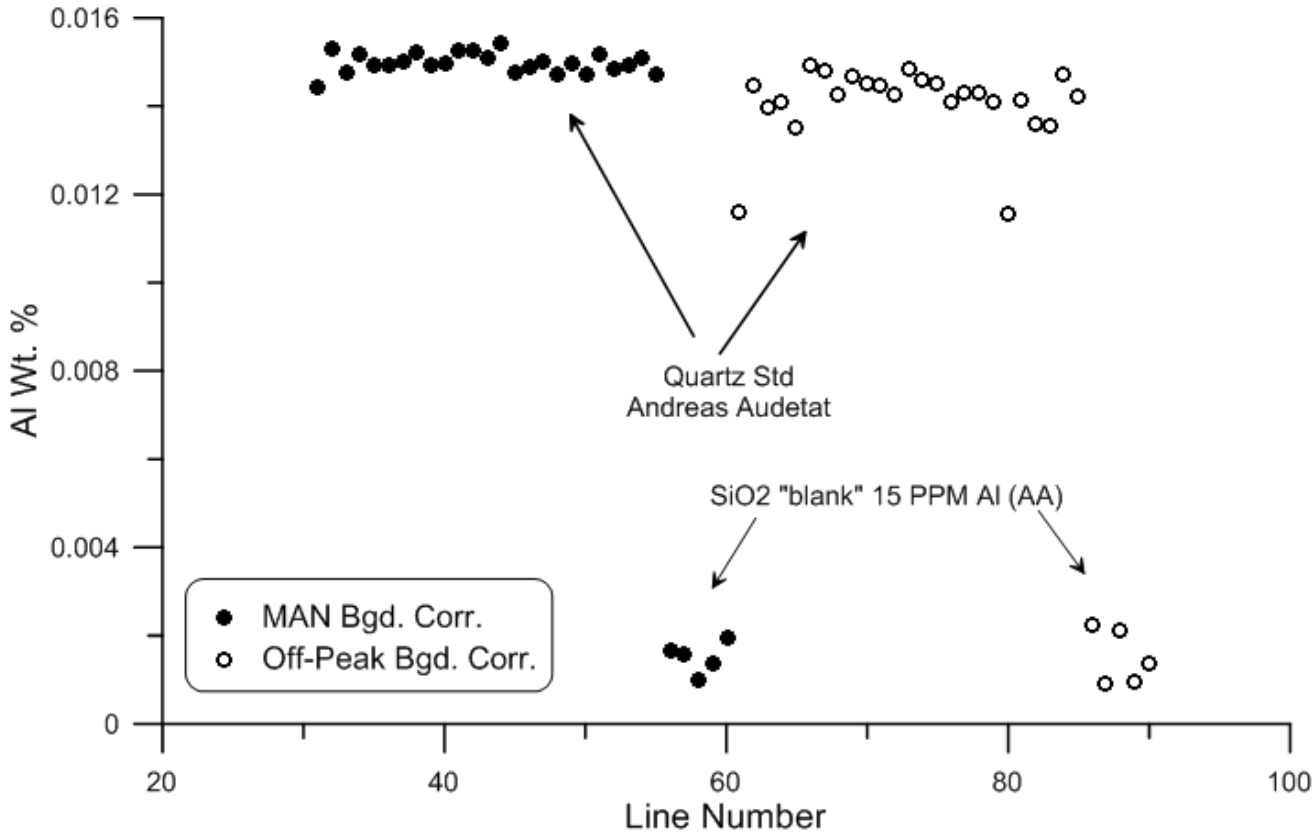

792

793 Fig 6. Al wt.% in Audetat natural quartz standard. MAN vs. Off-Peak, Al K□ (TAP/LTAP), 20
794 keV, 100 nA, 10 um, 200 secs on-peak, (200 secs off-peak). Both datasets are aggregates from 2
795 spectrometers and blank corrected. The line numbers are proxy for acquisition order and show
796 alternating acquisitions between off-peak and MAN measurements. Outliers on off-peak
797 measurements may represent spectrometer reproducibility problems that are not seen with MAN
798 measurements.

799
800
801

This is a preprint, the final version is subject to change, of the American Mineralogist (MSA)
Cite as Authors (Year) Title. American Mineralogist, in press.
(DOI will not work until issue is live.) DOI: http://dx.doi.org/10.2138/am-2016-5628

Revision 3

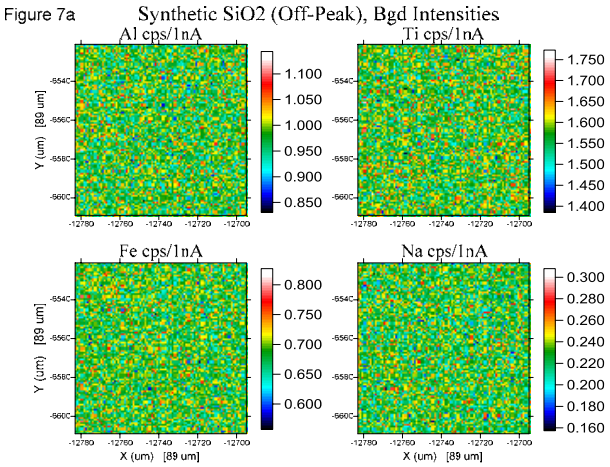

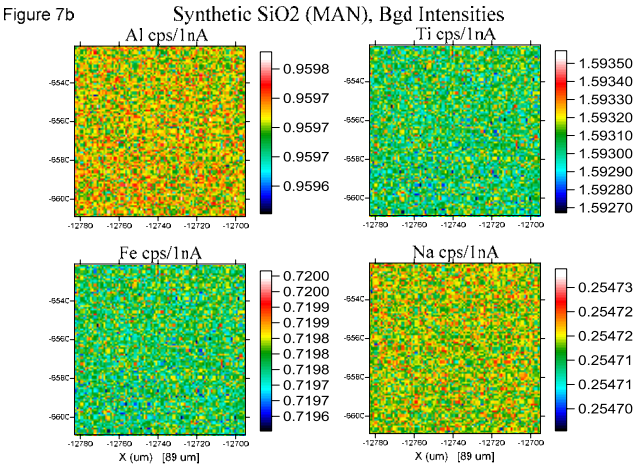

Fig. 7a. Calculated background intensities using a linear interpolation of the measured off-peak pixel intensities using high side and low side off-peak positions for Al,Kα, Ti Kα, Fe Kα and Na Kα in synthetic SiO_2, 15 keV, 100 nA, 6000 msec on-peak, 3000 msec off-peak (x2). Note that the calculated background intensities show the expected variance from the off-peak measurement uncertainties.

Fig. 7b. Calculated background intensities using a linear regression curve from the measured on-peak pixel intensities for a number of standard materials which **do not** contain the elements of interest. Al Kα, Ti Kα, Fe Kα and Na Kα in synthetic SiO_2, 15 keV, 100 nA, 6000 msec on-peak. Note that the calculated background intensities show a much smaller degree of variance. This is due to the fact that the MAN calibration curve always returns the same intensity value for a given average Z, which is based on the measured composition. Since the composition is this case (pure SiO_2) is essentially constant (the variation in the trace elements causes some small degree of calculated average Z), the calculated is also essentially a constant.

The fact that a re-measurement of the MAN regression curve will produce slightly different (but again essentially constant intensities for a given average Z), indicates an accuracy error that must be corrected using the blank correction step as described in the text.

This is a preprint, the final version is subject to change, of the American Mineralogist (MSA)
Cite as Authors (Year) Title. American Mineralogist, in press.
(DOI will not work until issue is live.) DOI: http://dx.doi.org/10.2138/am-2016-5628

Revision 3

Figure 8a

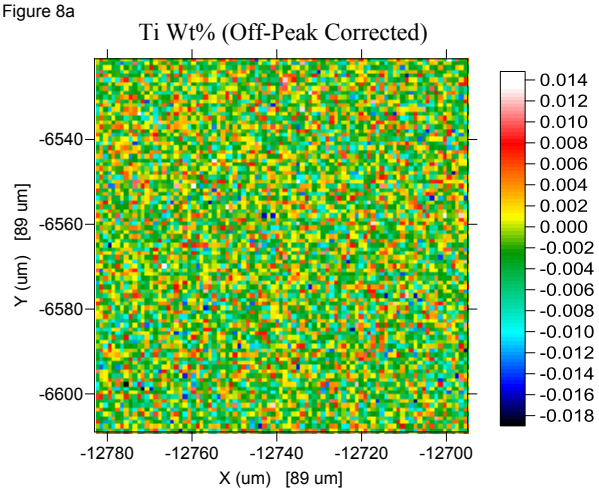

Figure 8b

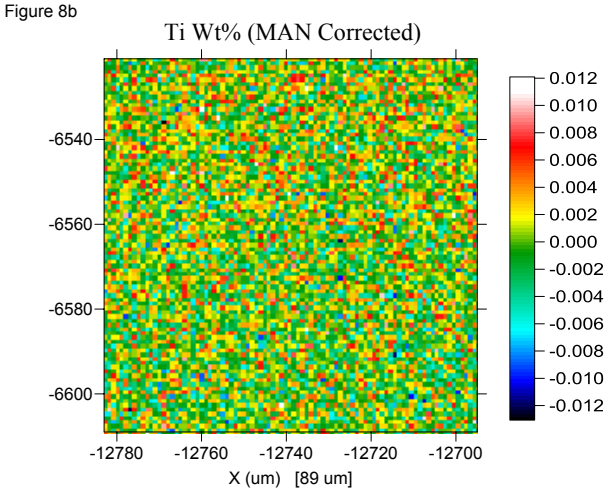

Fig. 8a. Ti wt.% in synthetic SiO_2, 15 keV, 100 nA, 6000 msec on-peak, 3000 msec off-peak (x2) and processed using measured off-peak backgrounds.

Fig. 8b. Ti wt.% in synthetic SiO_2, 15 keV, 100 nA, 6000 msec on-peak (only) and processed using measured MAN standard calibration curve in ½ the acquisition time (using the on-peak intensities from fig. 8a). The average (zero) difference between the two maps is approximately 20-30 PPM, without any "blank" correction".

This is a preprint, the final version is subject to change, of the American Mineralogist (MSA)
Cite as Authors (Year) Title. American Mineralogist, in press.
(DOI will not work until issue is live.) DOI: http://dx.doi.org/10.2138/am-2016-5628

Revision 3

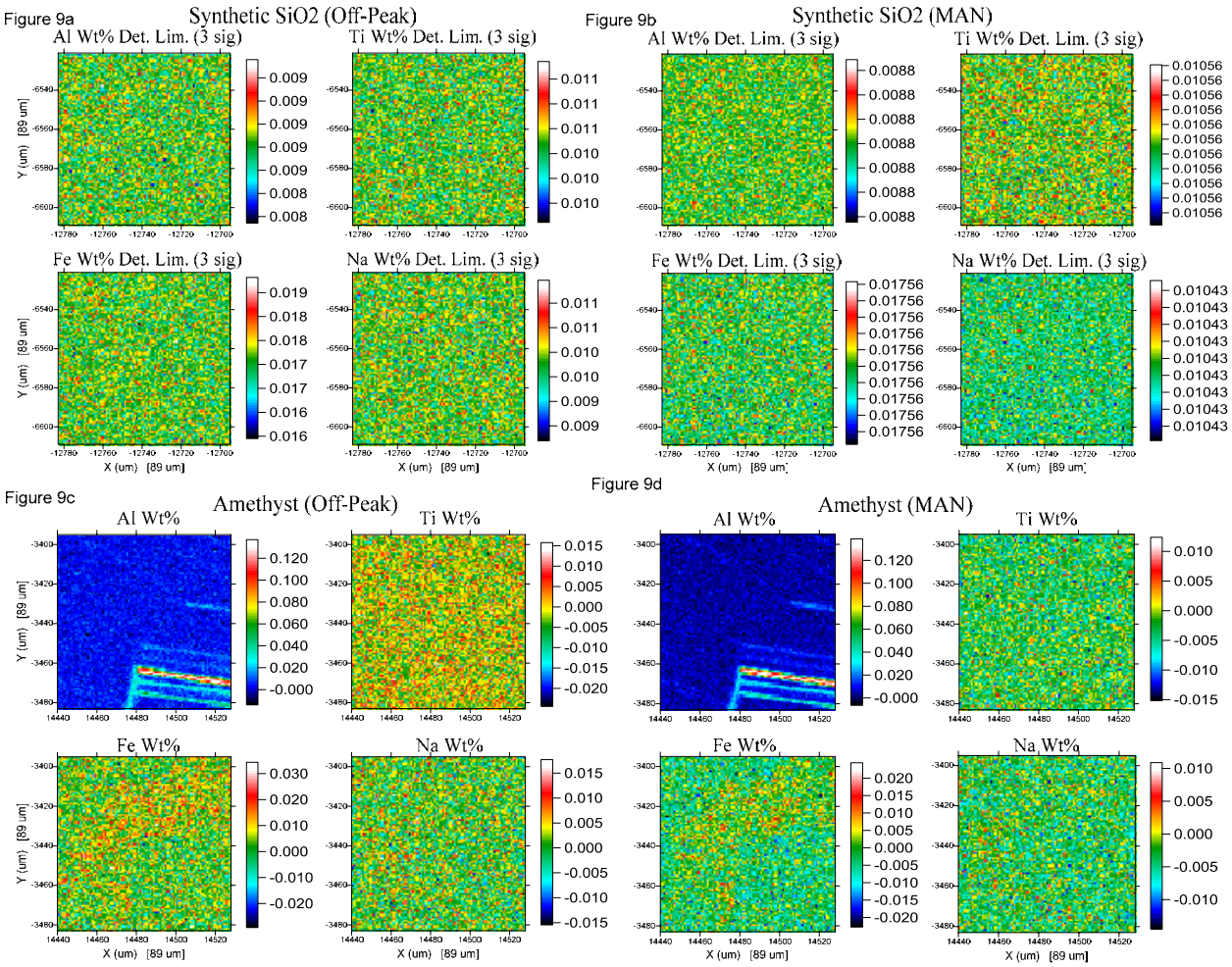

Fig. 9a. Calculated detection limits in synthetic SiO_2, 15 keV, 100 nA, 6000 msec, 3000 msec off-peak (x2) with off-peak processing and no blank correction. Off-peak sensitivity is a combination of both the on-peak and off-peak counting statistics.

Fig 9b. Calculated detection limits in synthetic SiO_2, 15 keV, 100 nA, 6000 msec on-peak only, MAN background correction and no blank correction. Because the MAN background method is dominated essentially by the on-peak counting statistics, we obtain better sensitivity in approximately ½ the counting time.

Fig 9c. Al, Ti, Fe and Na wt.% in Reed amethyst (Butte, MO), 15 keV, 100 nA, 6000 msec on-peak and 3000 msec off-peak (x2) using off-peak background corrections and blank corrected.

Fig. 9d. Al, Ti, Fe and Na wt.% in Reed amethyst (Butte, MO), 15 keV, 100 nA, 6000 msec on-peak using MAN (on-peak) intensities only and blank corrected.

This is a preprint, the final version is subject to change, of the American Mineralogist (MSA)
Cite as Authors (Year) Title. American Mineralogist, in press.
(DOI will not work until issue is live.) DOI: http://dx.doi.org/10.2138/am-2016-5628

Revision 3

Figure 10

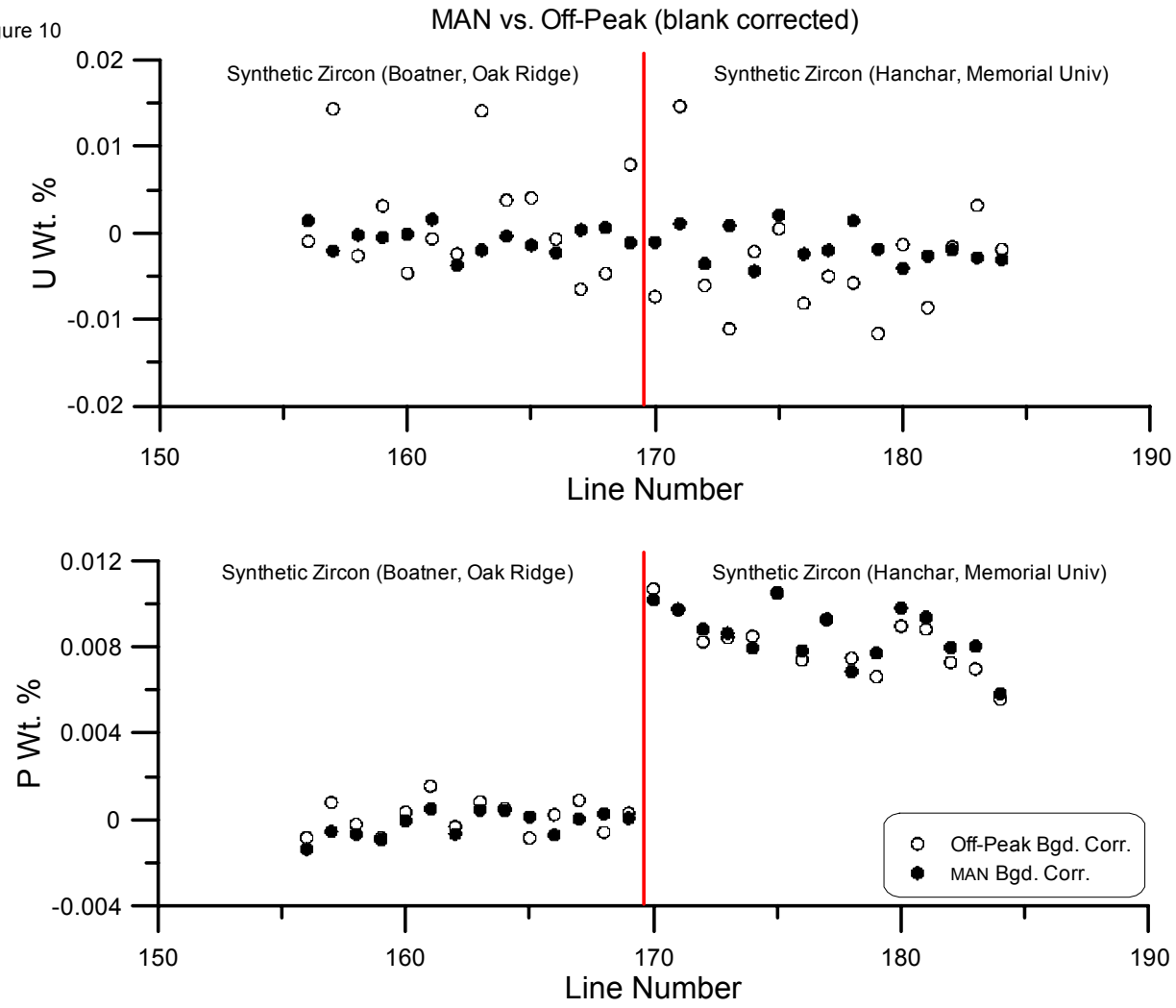

Fig 10. Point analyses on two synthetic zircons for both off-peak measured and MAN calculated background intensities for U and P. Acquisition conditions were 20 keV, 100 nA, 10 um, 200 secs on-peak, (200 secs off-peak). Note the somewhat larger variance in the off-peak data for U and what appears to be approximately 80 PPM of P in the Hanchar zircon compared to the Oak Ridge zircon.

This is a preprint, the final version is subject to change, of the American Mineralogist (MSA)
Cite as Authors (Year) Title. American Mineralogist, in press.
(DOI will not work until issue is live.) DOI: http://dx.doi.org/10.2138/am-2016-5628

Revision 3

Figure 11

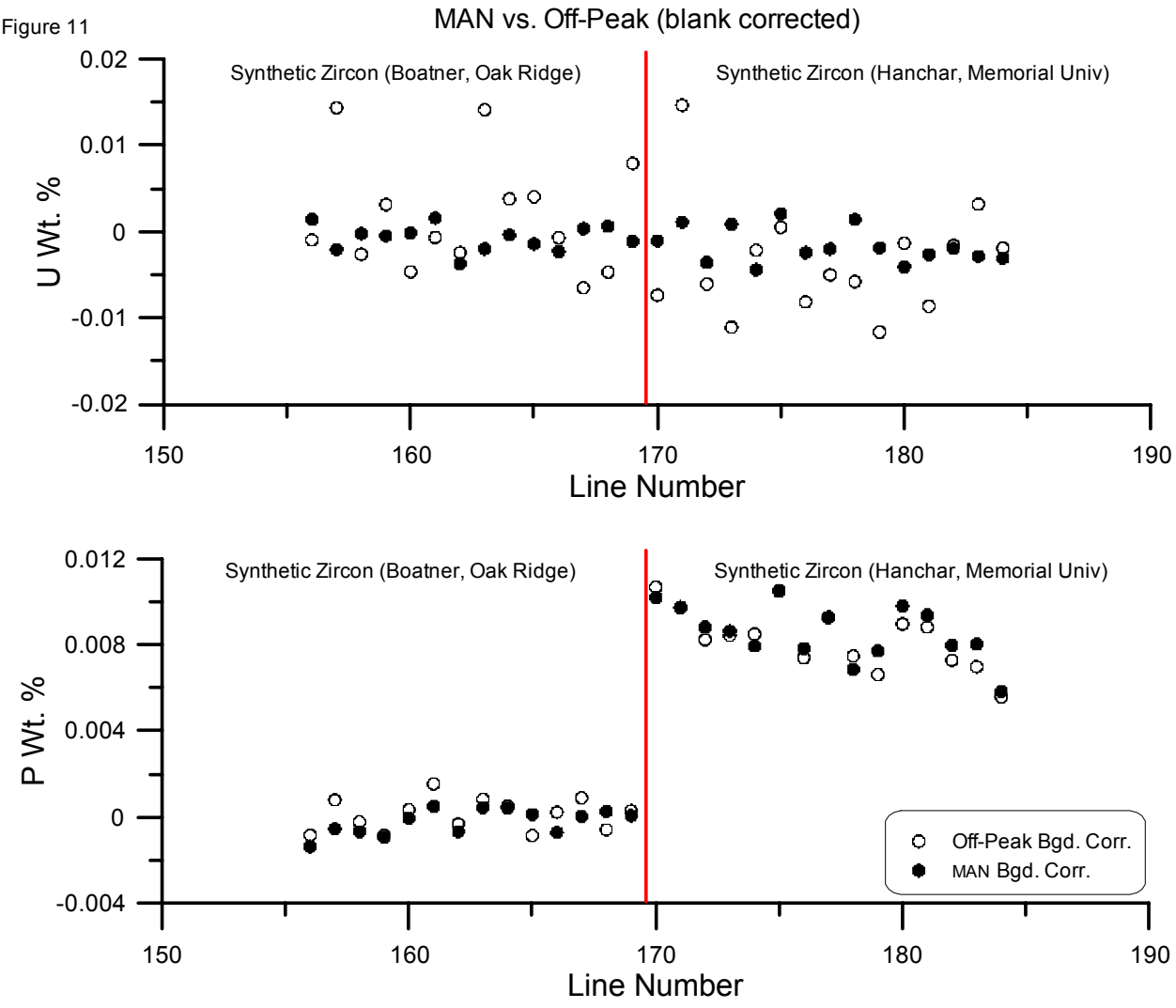

Fig 11. Point analyses (line profile with approximately 30 um spacing) on two synthetic zircons for both off-peak measured and MAN calculated background intensities for Th and Hf. Acquisition conditions were 20 keV, 100 nA, 10 um, 200 secs on-peak, (100 secs off-peak, x2). Although the concentrations and variances for these elements are similar for both background correction methods, use of the MAN background correction requires ½ the acquisition time of the traditional off-peak method.

This is a preprint, the final version is subject to change, of the American Mineralogist (MSA)
Cite as Authors (Year) Title. American Mineralogist, in press.
(DOI will not work until issue is live.) DOI: http://dx.doi.org/10.2138/am-2016-5628

Revision 3

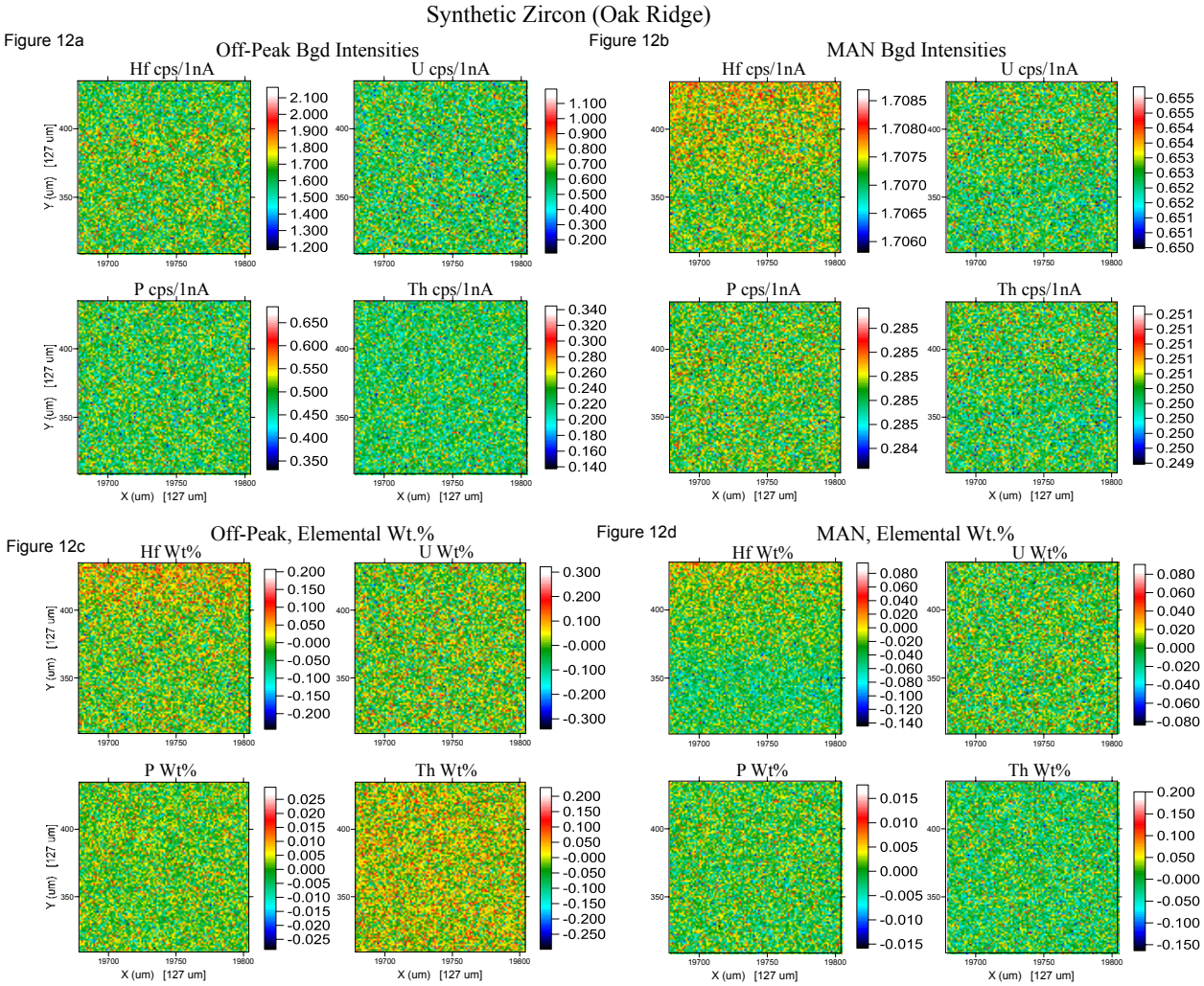

Fig. 12a. Calculated background intensities in a synthetic zircon (#257 from Lynn Boatner at Oak Ridge) using a linear interpolation of the measured off-peak pixel intensities using high side and low side off-peak positions for Hf Mα, U Mα, P Kα and Th Mα. Conditions were 20 keV, 100 nA, 3000 msec on-peak, 1500 msec off-peak (x2). Note that the calculated background intensities show the expected variance from the off-peak measurement uncertainties.

Fig. 12b. Calculated background intensities using a linear regression curve from the measured on-peak intensities for a number of standard materials which **do not** contain the elements of interest. Hf Mα, U Mα, P Kα and Th Mα, at 20 keV, 100 nA, 3000 msec on-peak only. Note that the calculated MAN background intensities show a much smaller degree of variance than the off-peak background intensities in Fig 12a. Also note that the calculated off-peak backgrounds in fig. 12a for P kα are much higher than the MAN calculated background intensities in this figure. This difference is due to significant interference from Zr L lines family on the P kα (low side) off-peak position. In other words, because MAN backgrounds do not utilize any off-peak data, there is no off-peak interferences for the MAN background method and hence a more accurate background correction in this case. Finally note the slightly greater concentration of Hf in the upper part of the map causes a slightly higher average Z to be calculated (and hence a slightly

higher MAN background intensity to be derived from the MAN calibration curve), which is only visible in the MAN background map.

Fig. 12c. Calculated elemental concentrations in a synthetic zircon using a linear interpolation from the measured off-peak intensities for Hf Mα, U Mα, P Kα and Th Mα. Conditions were 20 keV, 100 nA, 3000 msec on-peak, 1500 msec off-peak (x2) and blank corrected. Note that the calculated concentrations from the off-peak measurements show larger variations than the MAN background corrected intensities due to the variance of the off-peak measurements in fig 12a.

Fig. 12d. Calculated elemental concentrations in a synthetic zircon using MAN calibration curves corrected for continuum absorption for Hf Mα, U Mα, P Kα and Th Mα. Conditions were 20 keV, 100 nA, 3000 msec on-peak only and blank corrected. Note the variation in the Hf concentration map is significantly smaller for the MAN corrected map than the off-peak corrected map in fig 12c due to the greater precision of the MAN method.

This is a preprint, the final version is subject to change, of the American Mineralogist (MSA)
Cite as Authors (Year) Title. American Mineralogist, in press.
(DOI will not work until issue is live.) DOI: http://dx.doi.org/10.2138/am-2016-5628

Revision 3

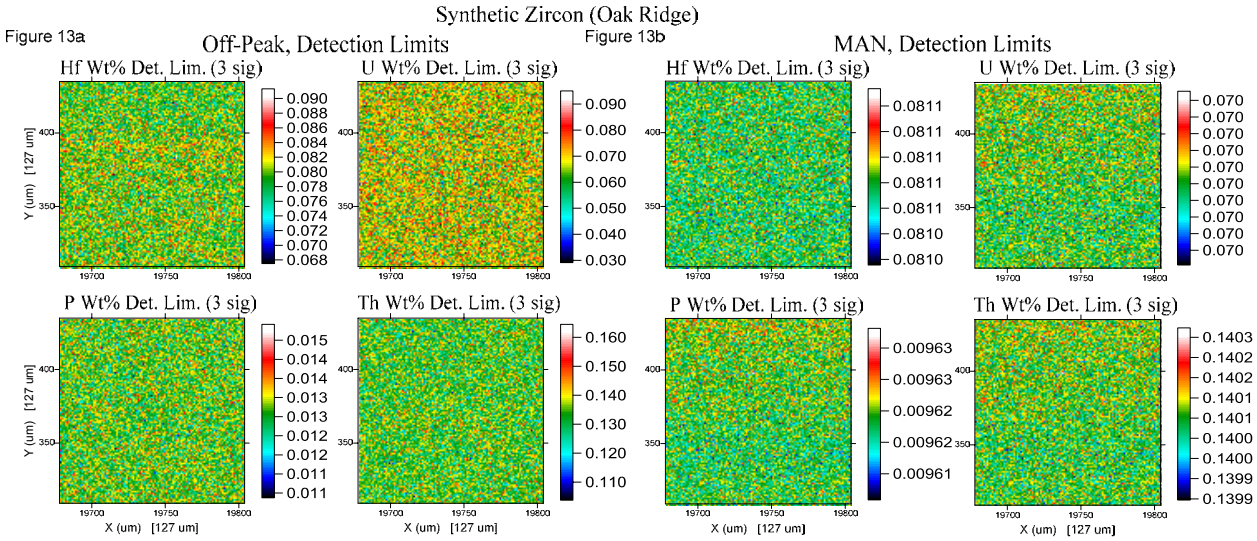

Fig 13a. Calculated detection limits in synthetic zircon (Boatner), 15 keV, 100 nA, 3000 msec, 1500 msec off-peak (x2) off-peak background correction without the blank correction. Off-peak sensitivity is a combination of on-peak and off-peak counting statistics

Fig 13b. Calculated detection limits in synthetic zircon (Boatner), 15 keV, 100 nA, 3000 msec on-peak only, MAN background correction and without a blank correction. The detection limit calculation in the case of the MAN background method is essentially dominated by only the on-peak counting statistics since the matrix elements are fixed by specification.

This is a preprint, the final version is subject to change, of the American Mineralogist (MSA)
Cite as Authors (Year) Title. American Mineralogist, in press.
(DOI will not work until issue is live.) DOI: http://dx.doi.org/10.2138/am-2016-5628

Revision 3

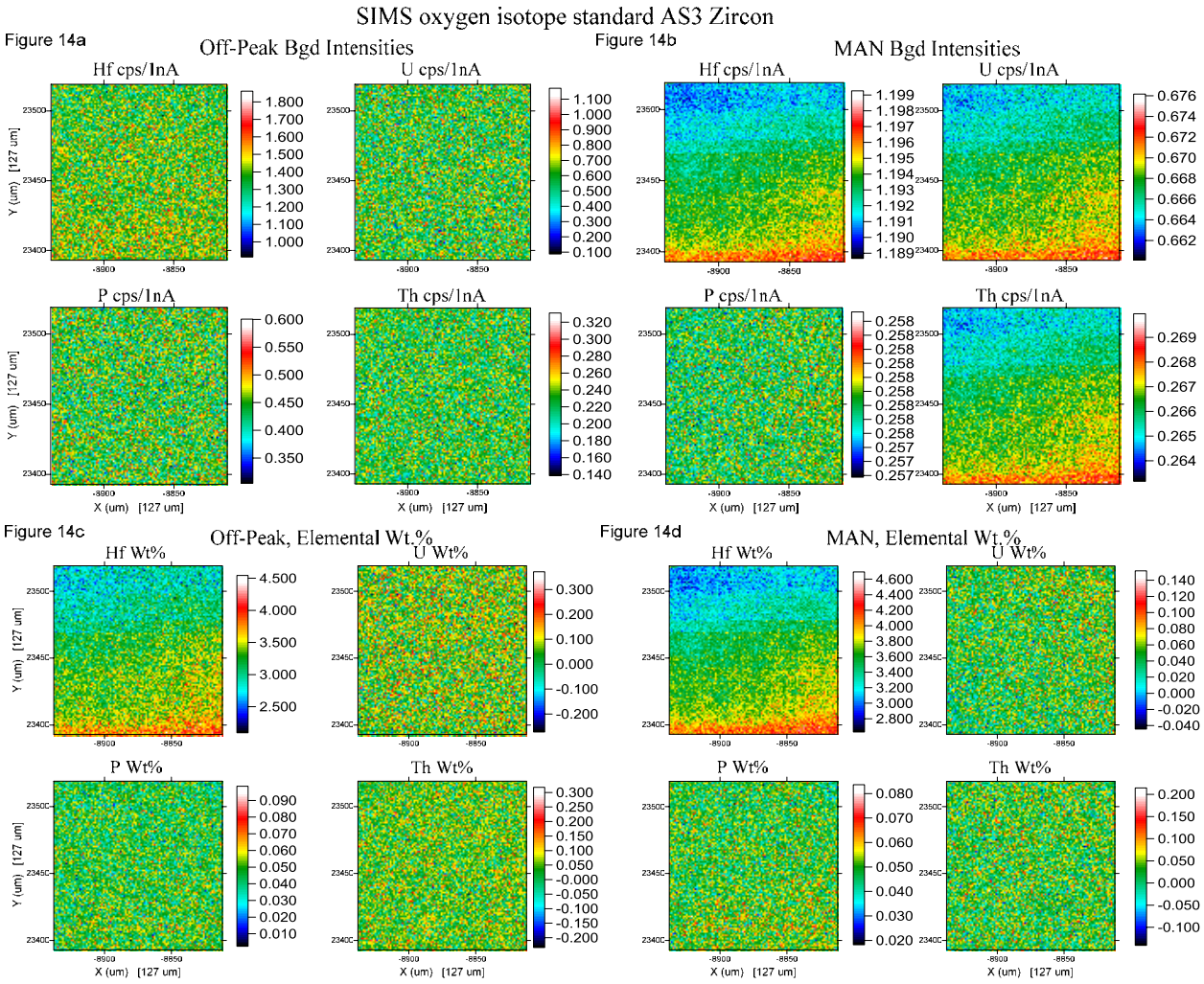

Fig. 14a. Calculated background intensities in SIMS oxygen isotope standard AS3 zircon using a linear interpolation from the measured off-peak intensities for Hf Mα, U Mα, P Kα and Th Mα. Conditions were 20 keV, 100 nA, 4000 msec on-peak, 2000 msec off-peak (x2).

Fig. 14b. Calculated background intensities in SIMS oxygen isotope standard AS3 zircon using MAN calibration curves corrected for continuum absorption for Hf Mα, U Mα, P Kα and Th Mα. Conditions were 20 keV, 100 nA, 4000 msec on-peak only. Note that the calculated MAN background intensities show a much smaller degree of variance than the off-peak background intensities in Fig 14a.

Fig. 14c. Calculated elemental concentrations in a natural SIMS oxygen isotope standard AS3 zircon using a linear interpolation from the measured off-peak intensities for Hf Mα, U Mα, P Kα and Th Mα. Conditions were 20 keV, 100 nA, 4000 msec on-peak, 2000 msec off-peak (x2). Note that the calculated concentrations for U and Th from these off-peak corrected measurements are consistently lower compared to the MAN background corrected concentrations as seen in fig. 14d, due to subtle interferences and continuum artifacts in the off-peak measurements.

929 Fig. 14d. Calculated elemental concentrations in a natural SIMS oxygen isotope standard AS3
930 zircon using MAN calibration curves corrected for continuum absorption for Hf Mα, U Mα, P
931 Kα and Th Mα. Conditions were 20 keV, 100 nA, 4000 msec on-peak only.
932

This is a preprint, the final version is subject to change, of the American Mineralogist (MSA)
Cite as Authors (Year) Title. American Mineralogist, in press.
(DOI will not work until issue is live.) DOI: http://dx.doi.org/10.2138/am-2016-5628

Revision 3

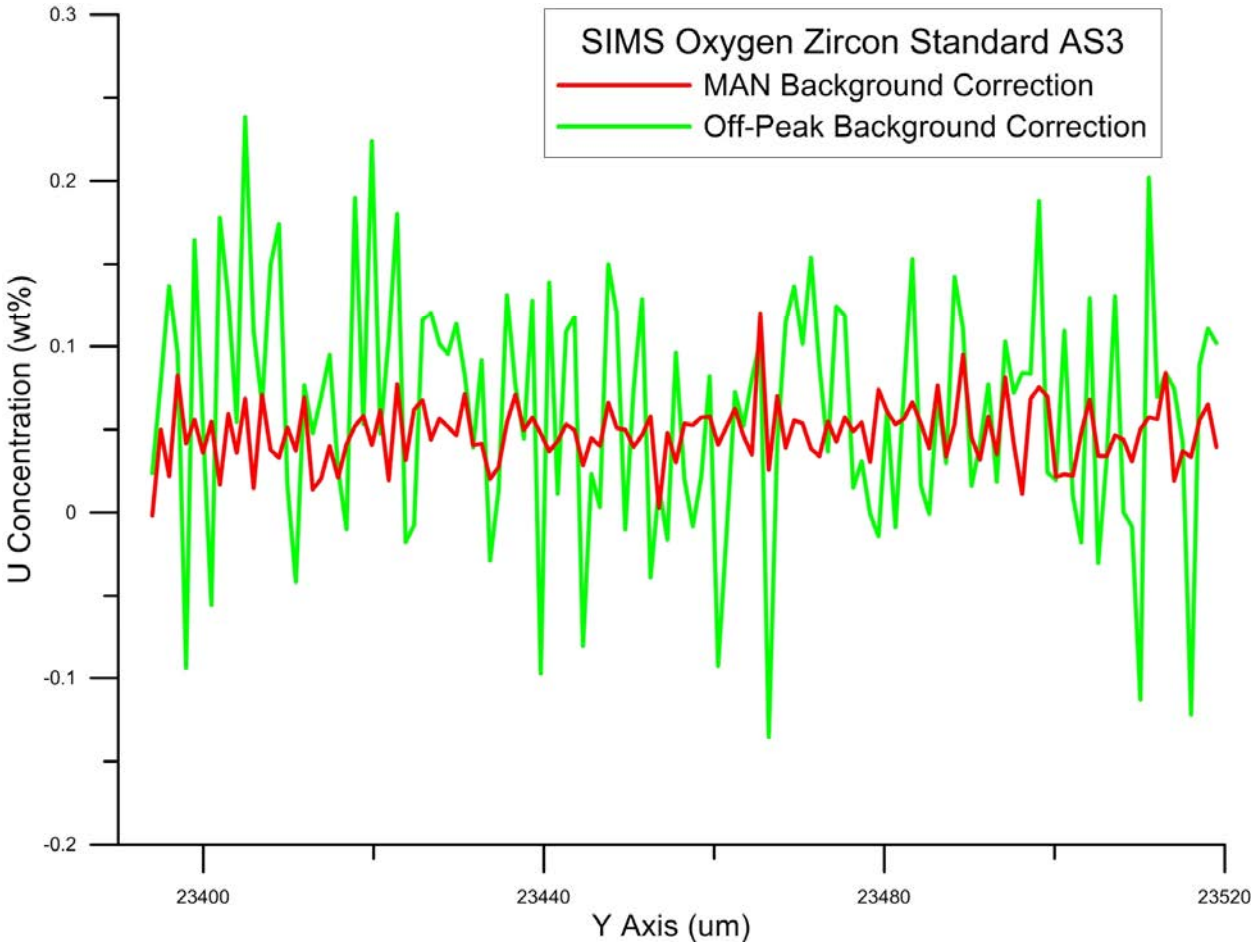

933

934 Fig. 15. Line profiles for both off-peak and MAN background methods for the U concentration
935 maps in figs 14c and 14d. Here we can easily see that accuracy is maintained and precision is
936 significantly improved, while in practice, the MAN method acquisition would take ½ the
937 acquisition time of the off-peak trace element maps.
938